Heat shock protein 90 relieves heat stress damage of myocardial cells by regulating Akt and PKM2 signaling *in vivo*

XIAO-HUI ZHANG, JIA-XIN WU, JUN-ZHOU SHA, BO YANG, JIA-RUI SUN and EN-DONG BAO

Department of Basic Veterinary Medicine, College of Veterinary Medicine, Nanjing Agricultural University, Nanjing, Jiangsu 210095, P.R. China

Received December 7, 2019; Accepted March 9, 2020

DOI: 10.3892/ijmm.2020.4560

Abstract. Heat shock protein 90 (Hsp90) is associated with resisting heat-stress injury to the heart, particularly in myocardial mitochondria. However, the mechanism underlying this effect remains unclear. The present study was based on the high expression of Hsp90 during heat stress (HS) and involved inducing higher expression of Hsp90 using aspirin in mouse hearts. Higher Hsp90 levels inhibited HS-induced myocardial damage and apoptosis, and mitochondrial dysfunction, by stimulating Akt (protein kinase B) activation and PKM2 (pyruvate kinase M2) signaling, and subsequently increasing mitochondrial Bcl-2 (B-cell lymphoma 2) levels and its phosphorylation. Functional inhibition of Hsp90 using geldanamycin verified that reducing the association of Hsp90 with Akt and PKM2 caused the functional decline of phosphorylated (p)-Akt and PKM2 that initiate Bcl-2 to move into mitochondria, where it is phosphorylated. Protection by Hsp90 was weakened by blocking Akt activation using Triciribine, which could not be recovered by normal initiation of the PKM2 pathway. Furthermore, increased Hsp70 levels induced by Akt activation in myocardial cells may flow into the blood to resist heat stress. The results provided *in vivo* mechanistic evidence that in myocardial cells, Hsp90 resists heat stress via separate activation of the Akt-Bcl-2 and PKM2-Bcl-2 signaling pathways, which contribute toward preserving cardiac function and mitochondrial homeostasis.

Introduction

Hot climates are becoming more apparent in recent years because of climate change and surges in temperature during the spring and summer months (1). The increase in body temperature caused by environmental heat exposure can result in heat stress (HS) and even sudden death (2,3), which has been reported frequently in studies in the United States and warm countries, such as Saudi Arabia (4,5). Previous studies have suggested that heat stress-induced sudden death involves heart failure (2) and arterial hypotension (6), which are caused by disruption of the function and structure of cardiomyocytes related to heat stress-induced damage to the myocardial contractile force and the blood circulation throughout the body (7). The results of our previous studies demonstrated that a rat heart cell line exposed to heat for 5 h presented disintegrated mitochondrial cristae, and even showed apoptosis and necrosis (8,9). Heat damage to myocardial cells is associated with increases in certain serum enzymes, such as lactate dehydrogenase (LDH), and an imbalance of the oxidation and antioxidant system (9).

Within cells exposed to heat stress, heat shock proteins (HSPs) have a protective role in maintaining protein homeostasis through their roles as molecular chaperones (10,11). On exposure to HS, heat shock factors (HSFs), particularly HSF-1, are released from their protein complexes and bind to the heat shock elements (HSEs) of target genes following undergoing modification and nuclear import, which regulates the transcription of various HSP genes (12,13). In our previous study, when myocardial cells were stressed for 5 h, levels of Hsp90α protein increased, implying its role in maintaining the homeostasis of heat-stressed cells (8). Hsp90 participates in numerous survival signaling pathways. For instance, its downstream target, protein kinase B (Akt) is activated by various receptors for growth factors and cytokines, and pyruvate kinase M2 (PKM2) interacts with Hsp90 to phosphorylate B-cell lymphoma 2 (Bcl-2) after H_2O_2 treatment (14,15). These two pathways are well characterized in the regulation of cellular anti-apoptosis by exerting antioxidant effects and inhibiting caspase-dependent pathways, thereby reducing cellular loss and myocardial injury. However, little is known regarding the specific influence of Hsp90 on these signaling pathways during heat stress.

Aspirin (ASA), a non-steroidal anti-inflammatory drug (NSAID) used to treat fever, is now well established in the prevention of cardiovascular disease (16,17). ASA lowers the temperature threshold needed to induce Hsp gene transcription and promotes thermotolerance (18). Our previous studies in chickens confirmed that pre-treatment with ASA (1 mg/kg)

Correspondence to: Professor En-Dong Bao, Department of Basic Veterinary Medicine, College of Veterinary Medicine, Nanjing Agricultural University, 1 Weigang, Xuanwu, Nanjing, Jiangsu 210095, P.R. China
E-mail: b_endong@njau.edu.cn

Key words: Hsp90, signaling pathway, heat stress, mitochondria, myocardial tissue

for 2 h could induce Hsp90 expression in heat-stressed chicken myocardial cells *in vivo* and *in vitro*, and that ASA's protective role may be weakened using the specific Hsp90 function inhibitor, geldanamycin (GA) (19,20). In the present study, ASA and GA were used to regulate the expression or function of Hsp90.

The present study aimed to confirm the protective effect of Hsp90 on mouse hearts, particularly in the first 5 h of HS, via its expression induction and functional inhibition. Furthermore, protection of the survival pathways associated with Hsp90's chaperone function were also identified in myocardial mitochondria.

Materials and methods

Animal treatment and sampling. C57BL/6JNju male mice (6 weeks old; 20-25 g) were purchased from Shanghai GenePharma Co., Ltd. First, 40 mice were divided randomly into four groups: The control (Con) group, ASA group, HS group, and ASA + HS group. The mice were raised conventionally for 1 week, and then used to assess the effect of ASA on myocardial tissues of heat-stressed mice: The ASA and ASA + HS groups were administered with ASA (Sigma Aldrich; Merck KGaA; dissolved in distilled water) by intragastric administration (1 mg/kg body weight) (19), while the Con and HS groups were treated with saline only. After 2 h of ASA treatment, the HS and ASA + HS groups were exposed to HS by rapidly increasing the air temperature from (25±1)˚C to (42±1)˚C in a phytotron, while maintaining the humidity at 75%, for 5 h; the Con and ASA groups were kept under normal conditions (25±1˚C, humidity 75%) for the same period.

Subsequently, another 40 mice were randomly divided into Con, GA, HS, and GA + HS groups. The GA and GA + HS groups were treated with GA (Beyotime Institute of Biotechnology); dissolved in dimethyl sulfoxide (DMSO) and diluted with distilled water; the DMSO concentration was <0.1% by intraperitoneal injection (50 mg/kg body weight), according to the manufacturer's protocol, while the Con and HS groups were treated with saline only. After 14 h of GA or saline treatment, the HS and GA + HS groups were exposed to heat stress for 5 h, while the Con and GA groups were kept under normal conditions.

Finally, 40 mice were randomly divided into groups of Con, TR, HS and TR + HS. The TR and groups were treated with Triciribine (Beyotime Institute of Biotechnology; dissolved in DMSO and diluted with distilled water; the DMSO concentration was <0.1%), according to the manufacturer's protocol (1 mg/kg body weight), while the Con and HS groups were treated with saline only. After 14 h of TR treatment, the HS and TR + HS groups were exposed to heat stress for 5 h, while the Con and TR groups were kept under normal conditions.

All mice were allowed *ad libitum* access to food and water during the experiment. After measuring physiological indices and anesthesia with diethyl ether (after the mice had fallen down and exhibited slow breathing, adequate anesthesia was further confirmed by the skin pain reflex), orbital blood was collected from the mice (~0.5 ml per mouse), prior to the mice being sacrificed via cervical dislocation, and samples of their heart tissues being taken. For each group, five ventricles were used to extract mitochondria, and another five were cut into two halves, of which one was used for morphological detection, and the other was used for molecular biological analysis. All animal experiments were performed according to the guidelines of the regional Animal Ethics Committee and were approved by the Institutional Animal Care and Use Committee of Nanjing Agricultural University.

Measurement of physiological indices. Non-invasive Pulse Oxygen Respiratory Monitors (MouseOx, Starr Life Sciences Corp.) were used to measure the physiological parameters of the mice, including heart rate, blood oxygenation content and respiratory rate, according to the manufacturer's protocol.

Serum biochemical analyses. Mouse blood samples were centrifuged at 4,000 x g for 5 min to obtain the serum, which was sent to Super Biotech Co., Ltd. to detect the activities of creatine kinase (CK), lactate dehydrogenase (LDH), and aspartate aminotransferase (AST). Serum Hsp70 levels were analyzed using the mouse Hsp70 ELISA kit (cat. no. ANG-E21510M, Angle Gene), according to the manufacturer's protocol.

Detection of the oxidation and antioxidant capacity. The antioxidant status of the tested mouse hearts was assessed by measuring the levels of glutathione peroxidase (GSH-PX) and catalase (CAT). Peroxidation was estimated by measuring the malondialdehyde (MDA) content. For these biochemical analyses, hearts from five randomly selected animals per group were used. All the aforementioned indices were determined using the GSH-PX assay kit (cat. no. A005-1-2), the CAT assay kit (cat. no. A007-1-1) and the MDA assay kit (cat. no. A003-1-2), all from Jiancheng, according to the manufacturer's protocol.

Histopathological evaluations. For histopathological and immunohistofluorescence analyses, ventricular tissues of five animals per group were selected and fixed in 10% neutral formalin solution at room temperature (RT) for at least 48 h. Serial 3-4 μm sections were cut, followed by embedding in paraffin. The tissue sections were then deparaffinized and stained with hematoxylin and eosin (H&E) at RT for 3 and 5 min, respectively. Tissue damage was evaluated under a light microscope at x400 magnification by two pathologists who were blinded to the treatments. Damage was scored as follows: No obvious pathological change (0 points), swelling of myocytes or mild degeneration (1 point), middle myocardial degeneration (2 points), serious myocardial degeneration (3 points), and necrosis or fracture of myocardial fiber and microvascular hyperemia (4 points).

Deparaffinized sections were rehydrated in 100, 100, 95, 95, 85 and 75% alcohol, followed by antigen retrieval by boiling at 98˚C and washing with phosphate buffer solution. Tissue sections were successively blocked with 0.1% Triton X-100 at RT for 20 min, and then with goat serum (AR0009, Boster Bio) at 37˚C for 30 min. The slides were then incubated with primary antibodies against Hsp70 and Hsp90 (cat. nos. ab79852 and ab2928, Abcam), Akt and PKM2 (cat. nos. 9272 and 3198, Cell Signaling Technology, Inc.) at a dilution of 1:50 overnight at 4˚C. After washing in phosphate-buffered saline with 0.05% Tween-20, the slides were incubated with the FITC and TRITC-conjugated secondary antibody (dilution, 1:50 and 1:3;

cat. no., BA1105 and BA1090, Boster Bio) at 37˚C for 1 h, and then stained with 2-(4-amidinophenyl)-1H-indole-6-carboxamidine (DAPI) at RT for 1 min. Images were acquired under a fluorescence microscope at a magnification of x400.

TdT-mediated dUTP nick-end labeling (TUNEL) to detect cell apoptosis. TUNEL staining was conducted using a kit (KGA7021; KeyGen Biotech. Co. Ltd.) on serial sections deparaffinized as mentioned above, according to the manufacturer's protocol. Nuclei were re-stained with hematoxylin at RT for 35 sec. The sections were mounted with neutral balsam and observed under a light microscope at a magnification of x400. Myocardial apoptotic nuclei appeared brown and non-apoptotic nuclei appeared blue. The percentage of apoptotic cells among the total cardiomyocytes was used as the apoptotic rate.

Measuring the mitochondrial membrane potential (MMP) and openness of permeability transition pores. Purified myocardial mitochondria were diluted to 0.25 g/l protein concentration. The mitochondrial absorbance (A520) was observed at 520 nm before and after adding 200 μmol/l $CaCl_2$. The difference of A520 max-A520 min represents the open level of the mitochondrial permeability transition pore (mPTP) (21).

The tissue mitochondria isolation kit (cat. no. C3606; Beyotime Institute of Biotechnology) was used to isolate mitochondria of heart tissue according to the manufacturer's protocol. A mitochondrial membrane potential detection kit with JC-1 (cat. no. C2006; Beyotime Institute of Biotechnology) was used to measure the MMP, according to the manufacturer's protocol. Briefly, 0.1 ml purified mitochondria (20 μg) was incubated with 0.9 ml of 5-times-diluted JC-1 staining solution for 20 min at 37˚C. The fluorescence intensity of mitochondrial JC-1 monomers (λex 490 nm, λem 530 nm) and aggregates (λex 525 nm, λem 590 nm) were detected using a monochromator microplate reader (Safire II; Tecan Group Ltd.). The MMP in each sample was calculated as the fluorescence ratio of red (i.e., aggregates) to green (i.e., monomers).

Protein extraction and western blotting analysis. Following the designated treatments, the collected mouse heart tissues and purified mitochondria from mouse heart tissues were frozen at -80˚C for protein extraction. Total proteins were extracted using lysis buffer (cat. no., CW2333, CWBio) containing 1% phenylmethylsulfonyl fluoride and quantified using a bicinchoninic acid assay kit. Equal amounts of proteins (20 μg) were mixed with 5X SDS sample buffer, boiled for 5 min, and then separated by 10% SDS-PAGE. The proteins were transferred onto nitrocellulose membranes after electrophoresis. The membranes were incubated with 5% skimmed milk at RT for 2 h, prior to being incubated with primary antibodies against the following: Hsp90α (dilution, 1:1,000; cat. no. ab2928), Hsp70 (dilution, 1:10,000; cat. no. ab79852) and COX IV (dilution, 1:1,000; cat. no. ab16056; all Abcam) Akt (dilution, 1:1,000; cat. no. 9272), PKM2 (dilution, 1:1,000; cat. no. 3198), HSF-1 (dilution, 1:1,000; cat. no. 4356), caspase-3 (dilution, 1:1,000; cat. no. 9662), cytochrome *c* (cyt *c*; dilution, 1:1,000; cat. no. 4272), Bcl-2 (dilution, 1:1,000; cat. no. 3498) and β-actin (dilution, 1:1,000; cat. no. 4967; all Cell Signaling Technology, Inc.), phosphorylated (p)-Akt (dilution, 1:500; cat. no. sc-377556) and p-Bcl-2 (dilution, 1:500; cat. no. sc-377576) from Santa Cruz Biotechnology, Inc. Subsequently, the membranes were incubated for 2 h with corresponding horseradish peroxidase-conjugated secondary antibodies (cat. nos. BA1051 and BA1055; dilution, 1:5,000; Wuhan Boster Biological Technology, Ltd.). Immunoreactive protein bands were visualized using an electrochemiluminescence substrate and a gel-imaging system (Tanon Science and Technology, Co., Ltd.) with Image Analysis software (version 1.46; National Institutes of Health).

Statistical analysis. Data are expressed as the mean ± standard deviation. Differences among groups were determined using one-way analysis of variance, followed by Duncan's multiple range test using SPSS 25.0 version (IBM Corp.). $P<0.05$ was considered to indicate statistically significant differences.

Results

Higher Hsp90 levels alleviate the heat-stress damage of mouse heart tissues. Whether ASA exerts a protective effect on mouse heat-stressed hearts was first investigated through the examination of physiological indices, serum markers and histopathology (Fig. 1). HS significantly increased the heart rate and respiratory rate of the tested mice, but significantly decreased their blood oxygen saturation ($P<0.01$). Additionally, ASA administration enhanced the heart rate to a higher degree during HS, accompanied by significantly higher blood oxygen saturation, compared with that in the HS group ($P<0.01$; Fig. 1A). Detection of myocardial injury-related enzymes (Fig. 1B) revealed that, compared to the Con group, HS raised the serum levels of CK, LDH and AST ($P<0.01$), which were higher than those in the ASA + HS group, especially for LDH and AST ($P<0.05$). Consistent with these results, histopathological observation (Fig. 1C and D) revealed that HS caused severe tissue damage, characterized by granular degeneration, necrosis and rupture of myocardial fibers, and a higher pathological score than that in the Con group. ASA administration ameliorated the HS-induced myocardial necrosis and rupture, and decreased the pathological score significantly. These results revealed that ASA effectively alleviated HS-induced damage to heart tissues.

Western blotting revealed that the Hsp90 level in heart tissues increased significantly ($P<0.05$) after 5 h of heat exposure (Fig. 1E). ASA treatment alone also increased the Hsp90 level. HS in addition to ASA (ASA + HS) further increased the Hsp90 level significantly ($P<0.01$), compared with that in the HS or ASA alone groups. These results suggested that higher Hsp90 levels induced by ASA were associated with the remission of heart damage during HS.

Hsp90 activates the Akt and PKM2 signaling pathways in myocardial tissues. Akt is a known client protein of Hsp90 that binds to the middle domain of Hsp90 (22). A previous study indicated that PKM2, a key apoptosis regulator under oxidative stress, is a target of Hsp90. Hsp90 can induce a conformational change to increase the function of PKM2 (15). Therefore, the levels of Akt, p-Akt, and PKM2 in the tested heart tissues were analyzed using western blotting (Fig. 2A). Compared with the Con group, ASA alone increased the Akt

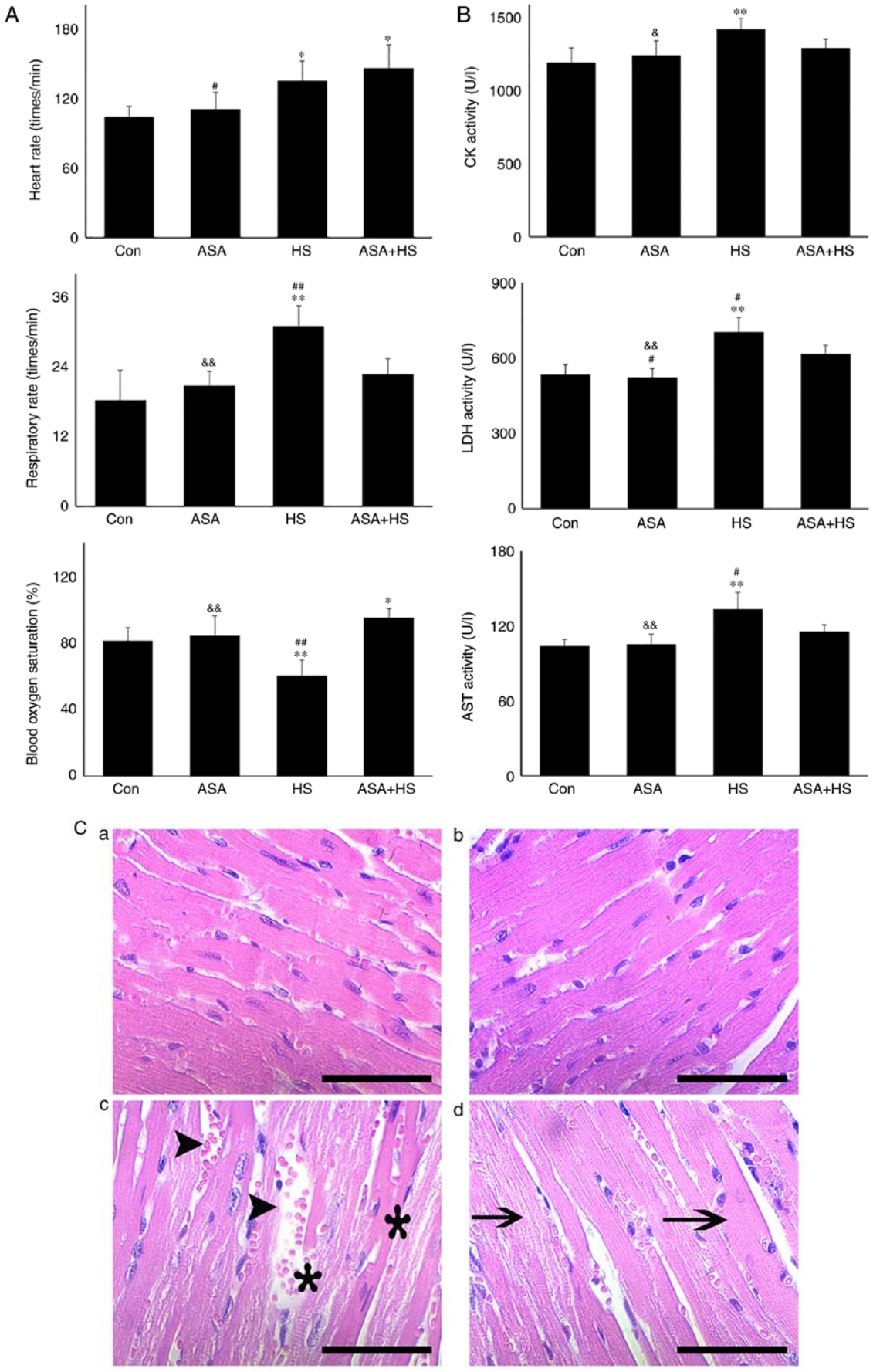

Figure 1. Effect of higher Hsp90 expression induced by ASA on heat-stressed heart tissues. (A) Effect of different Hsp90 expression levels on the heart rate, respiratory rate and blood oxygen saturation levels of mice. (B) Activities of enzymes associated with myocardial injury under different Hsp90 levels. (C) Representative H&E staining images of the histopathological examination from experimental mice are shown. Panels a-d represent the Con, ASA, HS, and ASA + HS groups, respectively. Scale bar=100 μm. Arrows indicate swelling cells and degeneration, the arrowhead points to hemorrhage, and asterisks mark necrosis and myofiber rupture.

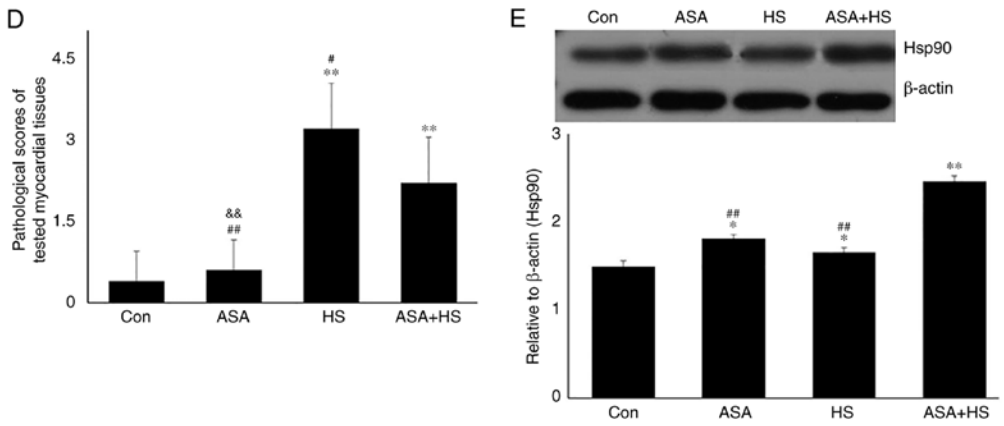

Figure 1. Continued. Effect of higher Hsp90 expression induced by ASA on heat-stressed heart tissues. (D) Pathological scores of the tested myocardial tissues. (E) Representative western blotting results for Hsp90 are shown. The relative abundance of Hsp90 was normalized to that of β-actin. All results are expressed as the mean ± SD; n=5. *P<0.05 and **P<0.01 vs. Con, $^{\#}$P<0.05 and $^{\#\#}$P<0.01 vs. ASA + HS, and the comparison between ASA and HS is indicated by $^{\&}$P<0.05 and $^{\&\&}$P<0.01.

level, which was further increased by ASA + HS administration. However, HS did not alter the Akt level. Additionally, compared with a slight increase in the p-Akt level in the HS group, ASA and ASA + HS administration further stimulated Akt phosphorylation, particularly in the ASA + HS group. However, the ratios of p-Akt to Akt in the ASA and ASA + HS groups were both decreased (P<0.01) but increased in the HS group. ASA treatment significantly upregulated the PKM2 level, regardless of the application of HS, while HS caused only a slight stimulation. Western blotting also revealed that, compared with the Con group, the Bcl-2 level was decreased following ASA treatment, accompanied by an increase in the p-Bcl-2 level. The p-Bcl-2 level in the HS group was lower than that in the ASA + HS group. Consistently, the ratios of p-Bcl-2 to Bcl-2 in the ASA and ASA + HS groups were decreased (P<0.01), but unchanged in the HS group.

Hsp90 stabilizes the conformation of client proteins or activates them, mainly depending on the binding of the N-terminal ATP binding domain and intermediate domain with client molecules (23). Therefore, the co-localization (potential interactions) of Hsp90 with Akt and PKM2 were detected using immunofluorescence staining (Fig. 2B). Co-localization of Hsp90 and Akt was not observed in the Con group. In the ASA and HS groups, co-localization between Hsp90 and Akt was detected, but only in the cytoplasm. In the ASA + HS group, the signal density of co-localization between Hsp90 and Akt was markedly increased in the cytoplasm. Notably, a certain amount of co-localization signal was also observed in the nucleus. Meanwhile, PKM2 in the Con group was mainly detected in the cytoplasm, with little in the nucleus, and there was little intracellular co-localization between Hsp90 and PKM2. In the ASA group, co-localization was markedly increased, together with an upregulated PKM2 level; however, the co-localization signal was still distributed only in the cytoplasm. In the HS group, the co-localization signal was slightly increased, and its nuclear translocation was observed. In the ASA + HS group, the co-localization between Hsp90 and PKM2 was markedly increased in the cytoplasm and nucleus, with an increased signal density to separate them, compared with that in the ASA or HS groups.

These data suggested that higher levels of Hsp90 induced by ASA promoted Akt expression and activation, and stimulated PKM2 signaling, possibly via their interaction, to exert the myocardial protective effect against HS, through the Bcl-2 phosphorylation.

Higher Hsp90 levels enhance the protection of mitochondria. Mitochondria are the most vulnerable organelles for intracellular injury. In the myocardium, HS results in cell peroxidation, inducing swelling of mitochondria, dilation of the mitochondrial inner cavity, and fracture of the mitochondrial ridge (24,25). The present study first evaluated intramitochondrial oxidative stress parameters in the different groups. HS significantly exacerbated the oxidative status, characterized by a decrease in GSH-PX, and increased CAT and MDA levels. Pre-induction of Hsp90 by ASA effectively strengthened the antioxidant capacity during HS through retaining higher GSH-PX and CAT activity, thereby decreasing the MDA level (Fig. 2C). An incomplete mitochondrial structure often results in the release of internal cyt *c*, which then activates caspase-3 and leads to the initiation of apoptosis (26). Our results revealed that higher levels of cyt *c* in the HS group corresponded to increased caspase-3 activation and a higher apoptosis rate of myocardial cells. Compared with those in the HS group, ASA treatment reduced the cyt *c* and caspase-3 levels during exposure to HS, and decreased the heat-stress-induced apoptosis rate (Fig. 2D and E). Consistently, HS induced further opening of the mPTP, and decreased the MMP, implying the structural failure and functional degradation of mitochondria. Higher Hsp90 levels in the ASA + HS group reversed these adverse trends, characterized by decreased opening of the mPTP and increased MMP (Fig. 2F). Taken together, these results suggested that the ASA-induced increase in Hsp90 could effectively reduce HS-related damage to mitochondria and secondary cellular apoptosis.

Hsp90 induced by ASA promotes p-Akt and PKM2 translocation into mitochondria. A previous study found that Akt activation in the cytoplasm alone was not sufficient to induce myocardial protection in mice with ischemia-reperfusion

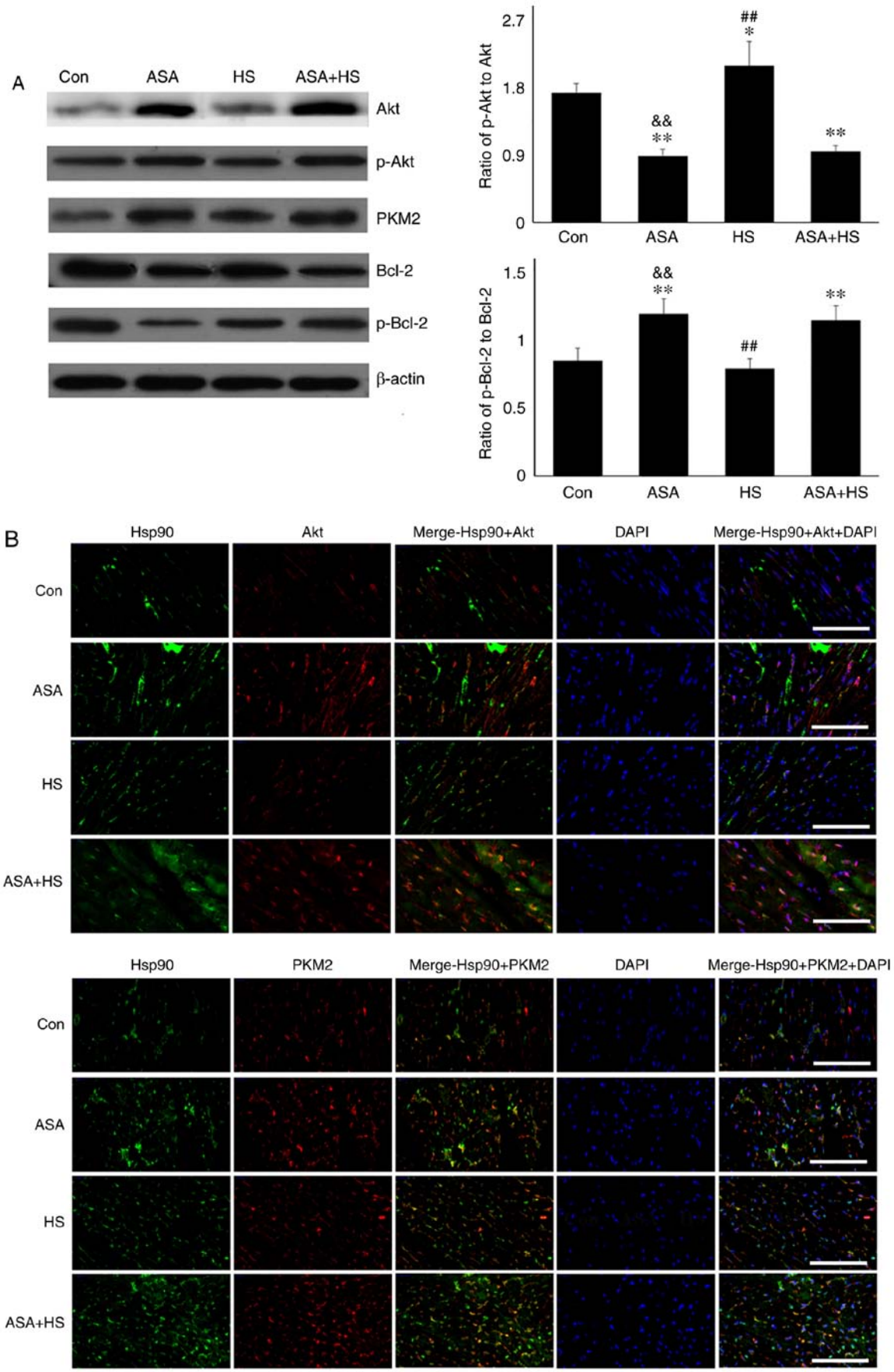

Figure 2. Effect of higher Hsp90 levels caused by ASA on the tested proteins, and the co-localization, apoptosis and mitochondria of myocardial cells. (A) Representative western blotting results for Akt, p-Akt, PKM2, Bcl-2 and p-Bcl-2 are shown, and the ratios of phosphorylated/total protein abundance are evaluated. (B) Representative immunohistofluorescence staining images showing the interaction between Hsp90 and Akt or PKM2 (Hsp90, green fluorescence; Akt/PKM2, red fluorescence; nucleus, blue fluorescence; the merged image of Hsp90 and Akt/PKM2 in the cytoplasm, yellow fluorescence; the merged image of Hsp90 and Akt/PKM2 in the nucleus, white fluorescence) in myocardial tissues.

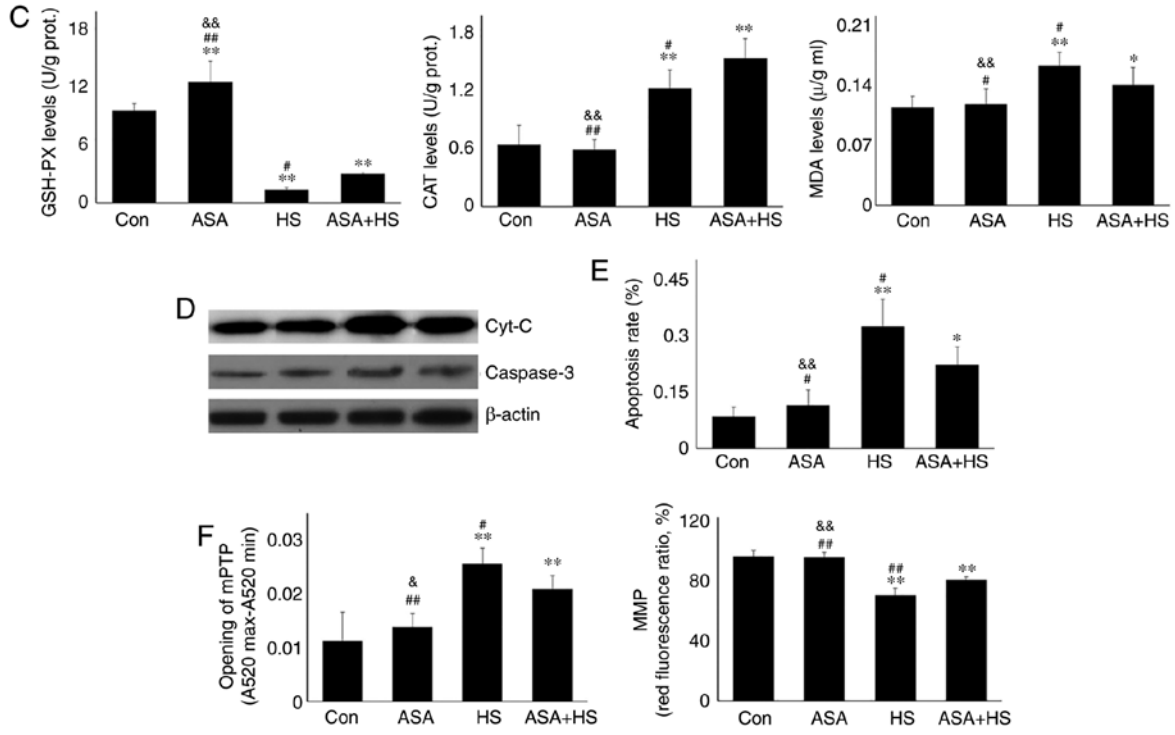

Figure 2. Continued. Effect of higher Hsp90 levels caused by ASA on the tested proteins, and the co-localization, apoptosis and mitochondria of myocardial cells. (C) Effect of higher Hsp90 abundance on the levels of GSH-PX, CAT and MDA. (D) Effect of higher Hsp90 abundance on the levels of cyt *c* and caspase-3. (E) The apoptotic rate of myocardial cells in the different groups. (F) The detection of myocardial mitochondrial function, mPTP and MMP, are shown. The results are expressed as the mean ± SD; n=5. *P<0.05 and **P<0.01 vs. Con, $^{\#}$P<0.05 and $^{\#\#}$P<0.01 vs. ASA + HS, and the comparison between ASA and HS is indicated by $^{\&}$P<0.05 and $^{\&\&}$P<0.01.

injury, and the translocation of phosphorylated Akt from the cytoplasm into the mitochondria was the key to inducing myocardial protection (27). However, the molecular mechanism of its anti-apoptotic effect remains unclear. A recent study showed that p-Bcl-2, the active form of Bcl-2 stimulated by Akt and PKM2, functions in the mitochondria (15). The results of the present study showed that HS upregulated the Hsp90, Akt, p-Akt and PKM2 levels significantly in the mitochondria of rat hearts. Compared with those in the HS group, in myocardial tissues of the ASA + HS group, higher Hsp90 levels led to markedly increased levels of these mitochondrial proteins (Fig. 3A). Meanwhile, the ratios of mitochondrial p-Akt to Akt in ASA, HS, and ASA + HS were all increased significantly, particularly in the ASA group (significantly higher than HS and ASA + HS). Western blotting revealed that mitochondrial Bcl-2 and p-Bcl-2 levels in the HS group were decreased compared with those in the Con group. Although the mitochondrial Bcl-2 levels also decreased markedly, the p-Bcl-2 level and the ratio of mitochondrial p-Bcl-2 to Bcl-2 were increased in the ASA group, and largely decreased in the ASA + HS, which was beneficial for resisting HS (Fig. 3B).

A previous study showed that the phosphatidylinositol-4,5-bisphosphate 3-kinase (PI3K)-Akt signaling pathway regulates Hsp70 expression by promoting HSF-1 expression and its nuclear translocation, which then critically contributes toward the chaperone function of Hsp90 through the interaction between Hsp70 and Hsp90 in multiple myeloma (28). The present study revealed that ASA and/or HS could effectively induce high levels of HSF-1 and Hsp70. The Hsp70 levels in the ASA and ASA + HS groups were also higher than those in the HS group (Fig. 3C). Immunohistofluorescence detection revealed no co-localization of Hsp70 and Hsp90 in the Con group, and although ASA treatment alone increased the Hsp70 and Hsp90 levels in the cytoplasm and nucleus, it did not promote their co-localization. HS induced a notable co-localization between Hsp70 and Hsp90 in the nucleus, while the co-localization in the ASA + HS group was notably higher than that in the HS group, based on of the higher levels and nuclear translocation of Hsp70 and Hsp90 (Fig. 3D).

Consistently, western blotting revealed that HS stimulated the cytosolic cyt *c* level in myocardial cells, despite no change in the mitochondria, thereby inducing higher levels of cytosolic caspase-3 and cellular apoptosis, compared with that in the Con group. The cytosolic cyt *c* level in the ASA + HS group was downregulated despite an increase in mitochondria, which only caused a lower caspase-3 activity and cellular apoptosis when compared with that in the HS group (Fig. 3E and F). These results suggested that increased Hsp90 levels could accelerate the mitochondrial translocation of p-Akt and PKM2, leading to phosphorylation of mitochondrial Bcl-2 to protect the integrity of mitochondria from apoptosis initiation.

Inhibition of Hsp90 function aggravates the heat-stress injury of mouse hearts. To confirm the protective role of Hsp90-mediated signaling against HS, GA was used to inhibit the function of Hsp90. Western blotting revealed that GA efficiently inhibited the function of Hsp90 in mouse hearts, characterized by marked increases in Hsp70 and HSF-1

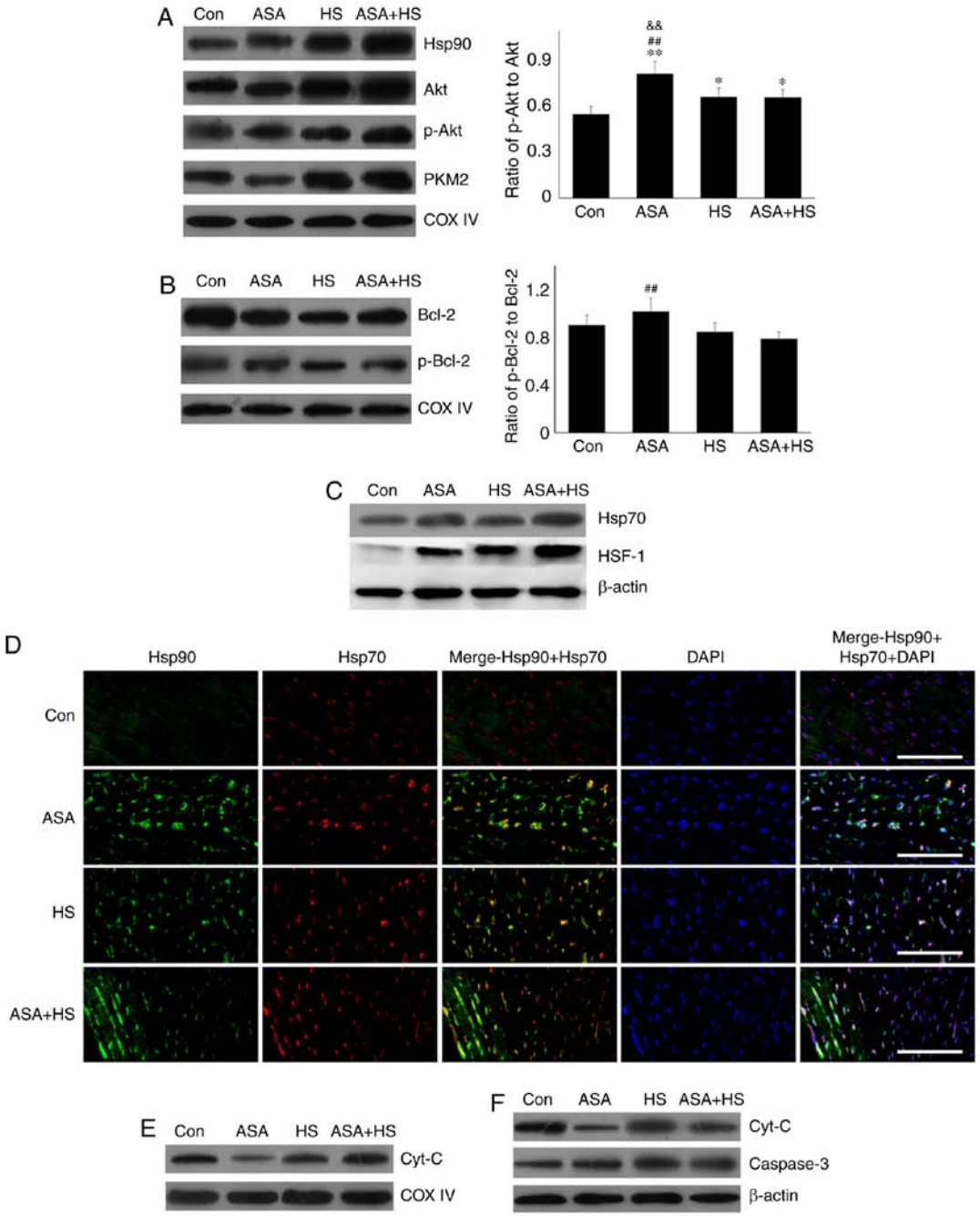

Figure 3. Effect of higher Hsp90 levels following ASA treatment on the mitochondrial proteins and the influence of intracellular Hsp70 on Hsp90. (A) Representative western blotting results of mitochondrial HSP90, Akt, p-Akt and PKM2 are shown, and the ratios of phosphorylated/total protein abundance are presented. (B) Representative western blotting results of mitochondrial Bcl-2 and p-Bcl-2, and the ratios of phosphorylated/total protein abundance are shown. (C) Representative western blotting results of cellular Hsp70 and HSF-1 are shown. (D) Representative immunohistofluorescence staining images showing the co-localization between Hsp90 and Hsp70 (Hsp90, green fluorescence; Hsp70, red fluorescence; nucleus, blue fluorescence; the merged image of Hsp90 and Hsp70 in the cytoplasm, yellow fluorescence; the merged image of Hsp90 and Hsp70 in the nucleus, white fluorescence) in myocardial tissues. Scale bar=100 μm. (E) Representative western blotting results of mitochondrial cyt *c* are shown. (F) Representative western blotting results of cytosolic cyt *c* and caspase-3 are shown. The results are expressed as the mean ± SD; n=5. *P<0.05 and **P<0.01 vs. Con, $^{\#\#}$P<0.01 vs. ASA + HS, and the comparison between ASA and HS is indicated by $^{\&\&}$P<0.01.

levels in the GA group, despite no change in the Hsp90 level (Fig. 4A) (29,30). Compared with those in the HS group, inhibition of Hsp90 in the GA + HS group caused a sharp downregulation of Hsp90 and HSF-1 levels, and an increase in Hsp70 levels, during heat stress. GA treatment decreased the ratios of p-Akt to Akt in GA and GA + HS groups, despite upregulation of the Akt level and its activation. Inhibition of Hsp90 caused PKM2 levels to accumulate in the GA group, which was also observed in the GA + HS group. GA decreased the levels of Bcl-2 and p-Bcl-2, including the ratios of p-Bcl-2 to Bcl-2, and treatment with HS and GA further exacerbated this effect. Immunohistofluorescence analysis (Fig. 4B) suggested that the merged signal of Hsp90 and Akt was slightly increased in the GA group. In addition, in the GA + HS group, the merged signal of Hsp90 and Akt was weakened and centralized around the nucleus. Co-localization of Hsp90

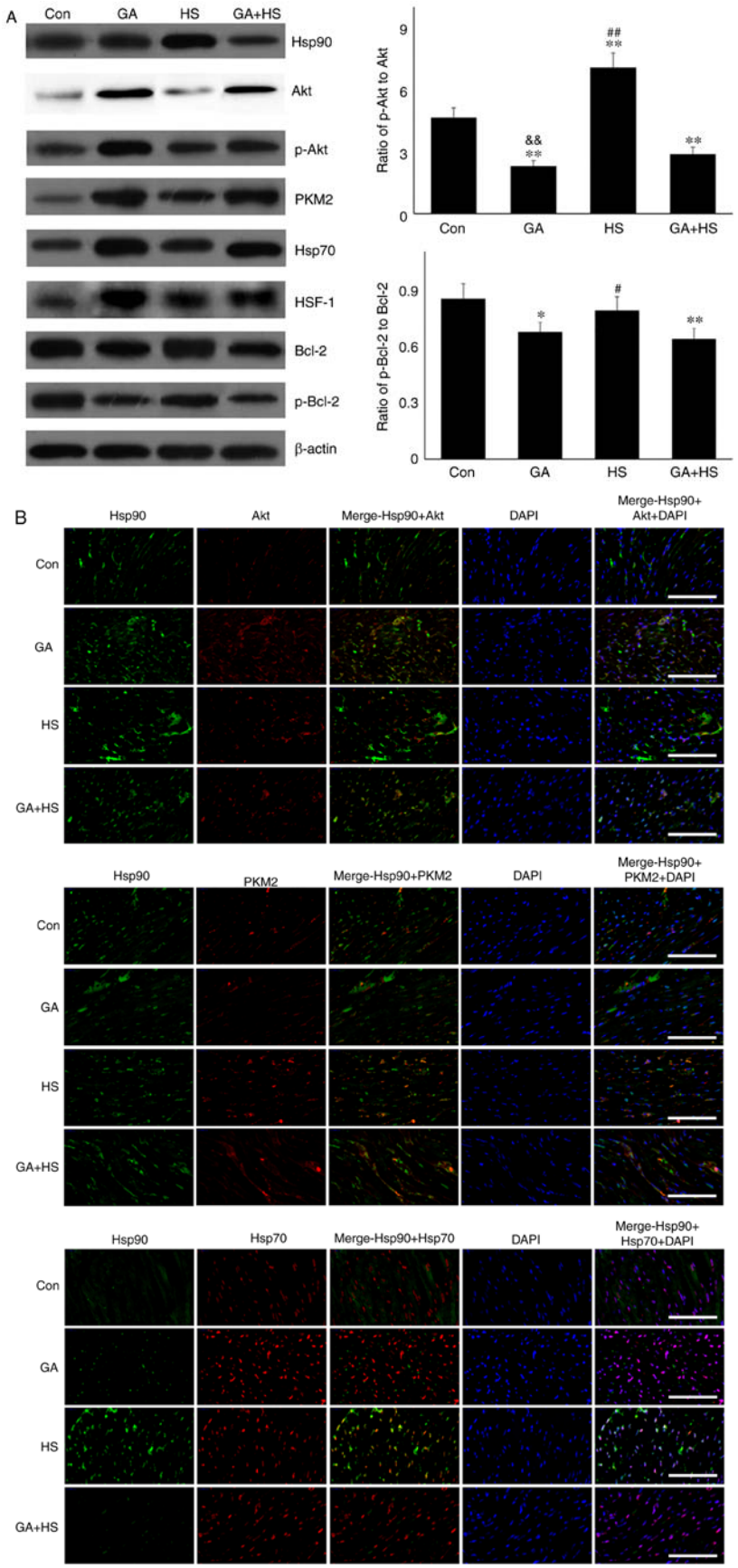

Figure 4. Effect of Hsp90 functional inhibition on the levels of Hsp90, its associated proteins, and the co-localization of Hsp90 with tested client proteins. (A) Representative western blotting results for cellular Hsp90, Akt, p-Akt, PKM2, Hsp70, HSF-1, Bcl-2 and p-Bcl-2 are shown, and the ratios of phosphorylated/total protein abundance are also presented. (B) Representative immunohistofluorescence staining images showing the co-localization of Hsp90 with Akt, PKM2 and Hsp70 (Hsp90, green fluorescence; Akt/PKM2/Hsp70, red fluorescence; nucleus, blue fluorescence; the merged image of Hsp90 and Akt/PKM2/Hsp70 in the cytoplasm, yellow fluorescence; the merged image of Hsp90 and Akt/PKM2/Hsp70 in the nucleus, white fluorescence) in myocardial tissues. Scale bar=100 μm. The results are expressed as the mean ± SD; n=5. *P<0.05 and **P<0.01 vs. Con, $^{\#}$P<0.05 and $^{\#\#}$P<0.01 vs. ASA + HS, and the comparison between ASA and HS is indicated by $^{\&\&}$P<0.01.

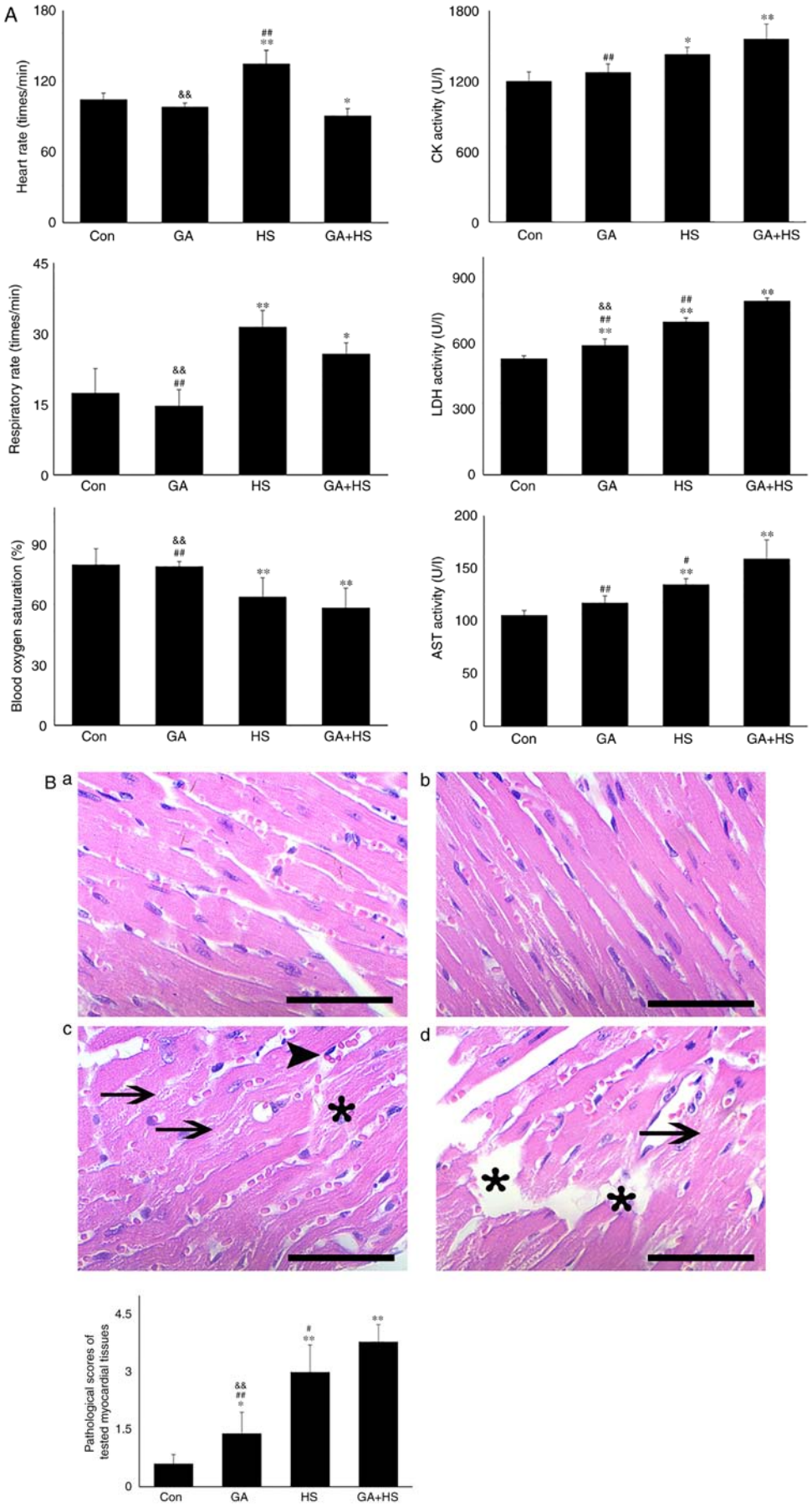

Figure 5. Effect of Hsp90 functional inhibition on the levels of myocardial injury and apoptosis. (A) Effect of Hsp90 functional inhibition on physiological indices, such as heart rate, respiratory rate and blood oxygen saturation, and enzymes activities associated with myocardial damage. (B) Representative images showing H&E staining for histopathological examination and its scores. Panels a-d represent the Con, GA, HS, and GA + HS groups, respectively. Arrows indicate swelling cells and degeneration, arrowheads point to hemorrhage, and asterisks mark necrosis and myofiber rupture. Scale bar=100 μm.

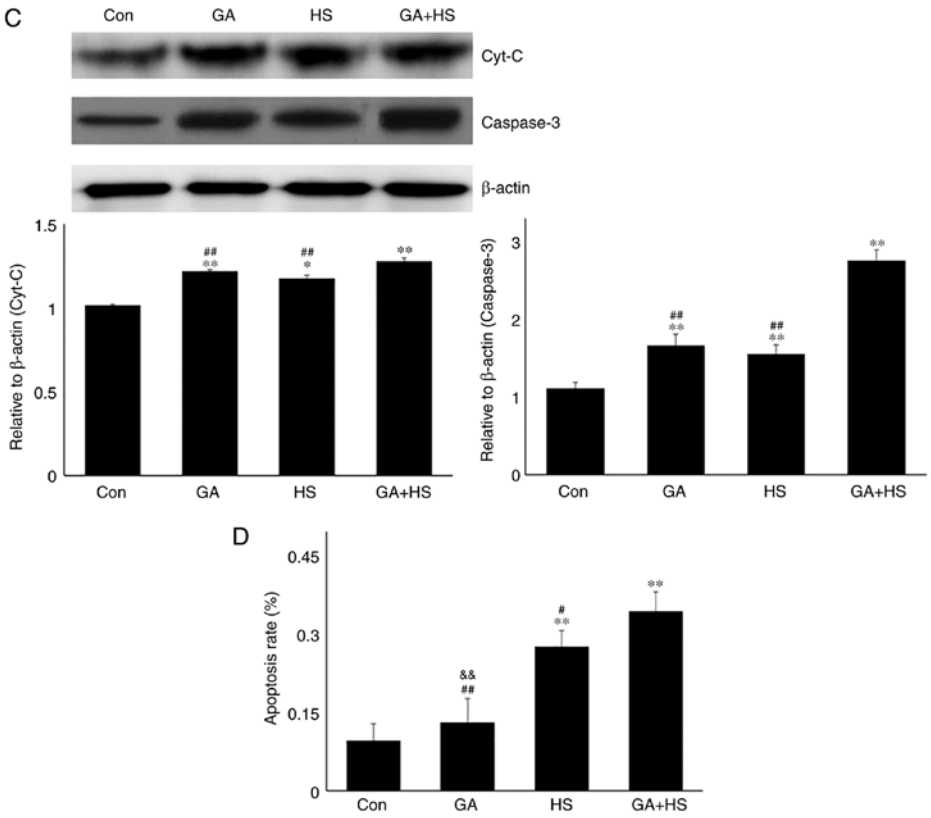

Figure 5. Continued. Effect of Hsp90 functional inhibition on the levels of myocardial injury and apoptosis. (C) Effect of Hsp90 functional inhibition on the cyt *c* and caspase-3 levels in heart tissues. (D) Apoptosis rate of myocardial cells under different treatments. The relative abundance of all proteins was normalized to that of β-actin. All the results are expressed as the mean ± SD; n=5. *P<0.05 and **P<0.01 vs. Con, $^{\#}$P<0.05 and $^{\#\#}$P<0.01 vs. ASA + HS, and the comparison between ASA and HS is indicated by $^{\&\&}$P<0.01.

and PKM2 was observed in the HS group, but not in the GA group, while in the GA + HS group, co-localization of Hsp90 and PKM2 could be detected in the cytoplasm and nucleus, but was weaker compared with that in the HS group. A clear co-localization signal of Hsp70 and Hsp90 was detected in the HS group, but not in the GA and GA + HS groups.

In consideration of the aforementioned results, the physiological indices, damage level and apoptosis of mouse hearts were examined. GA did not alter the heart rate, respiratory rate or blood oxygen saturation significantly. Compared with that in the HS group, the heart rate was markedly decreased in the GA + HS group (P<0.01), while the respiratory rate and blood oxygen saturation were also slightly inhibited (Fig. 5A). Biochemical analysis revealed that GA treatment increased the serum LDH level, but CK and AST levels, and compared with those in the HS group, whereas GA + HS further stimulated the release of LDH and AST into the blood during HS exposure (P<0.01 and P<0.05; Fig. 5A). H&E staining also showed that GA pre-treatment aggravated the HS-induced damage to myocardial tissues, indicated by increased myocardial rupture and a higher injury score (Fig. 5B). TUNEL staining (Fig. 5C and D) revealed that the inhibition of Hsp90 by GA increased HS-induced apoptosis (P<0.05), compared with that in the HS group. Furthermore, GA alone increased the levels of cyt *c* and caspase-3, and HS further enhanced the induction of cyt *c* and caspase-3. These results implied that Hsp90 was involved in the anti-damage response in heat-stressed mouse hearts, and that this damage may be associated with the reduced interaction of Hsp90 with Akt, PKM2 and Hsp70, resulting in decreased Akt and Bcl-2 activation.

Inhibition of Hsp90 function restricts the mitochondrial protection of Akt and PKM2. To confirm whether the functional deficiency of Hsp90 influenced the mitochondrial effect of Akt and PKM2 against HS *in vivo*, mitochondria from all related groups were isolated and studied. As shown in Fig. 6A, the mitochondrial Hsp90 level was increased by GA treatment to compensate for its functional insufficiency. Meanwhile, in addition to Akt and p-Akt, the PKM2 levels in the myocardial mitochondria were also increased in response to GA, regardless of heat stress. Due to the loss of chaperone protection of Hsp90 on Akt, the ratio of mitochondrial p-Akt to Akt increased in the GA group, which was further increased in the GA + HS group. However, western blotting revealed that the inhibition of Hsp90 by GA markedly antagonized the levels of mitochondrial Bcl-2 and p-Bcl-2. Notably, compared with that in the HS group, the mitochondrial p-Bcl-2 level in the GA + HS group remained markedly restrained, consistent with the ratio of p-Bcl-2 to Bcl-2. These implied that Hsp90 did not affect the mitochondrial translocation of Akt and PKM2 directly; however, it was responsible for p-Akt and PKM2 assisting Bcl-2 in entering into mitochondria and the initiation of its phosphorylation.

Western blotting (Fig. 6B) revealed that GA treatment markedly increased the mitochondrial cyt *c* level, but not the cytosolic cyt *c* level. HS following GA treatment increased

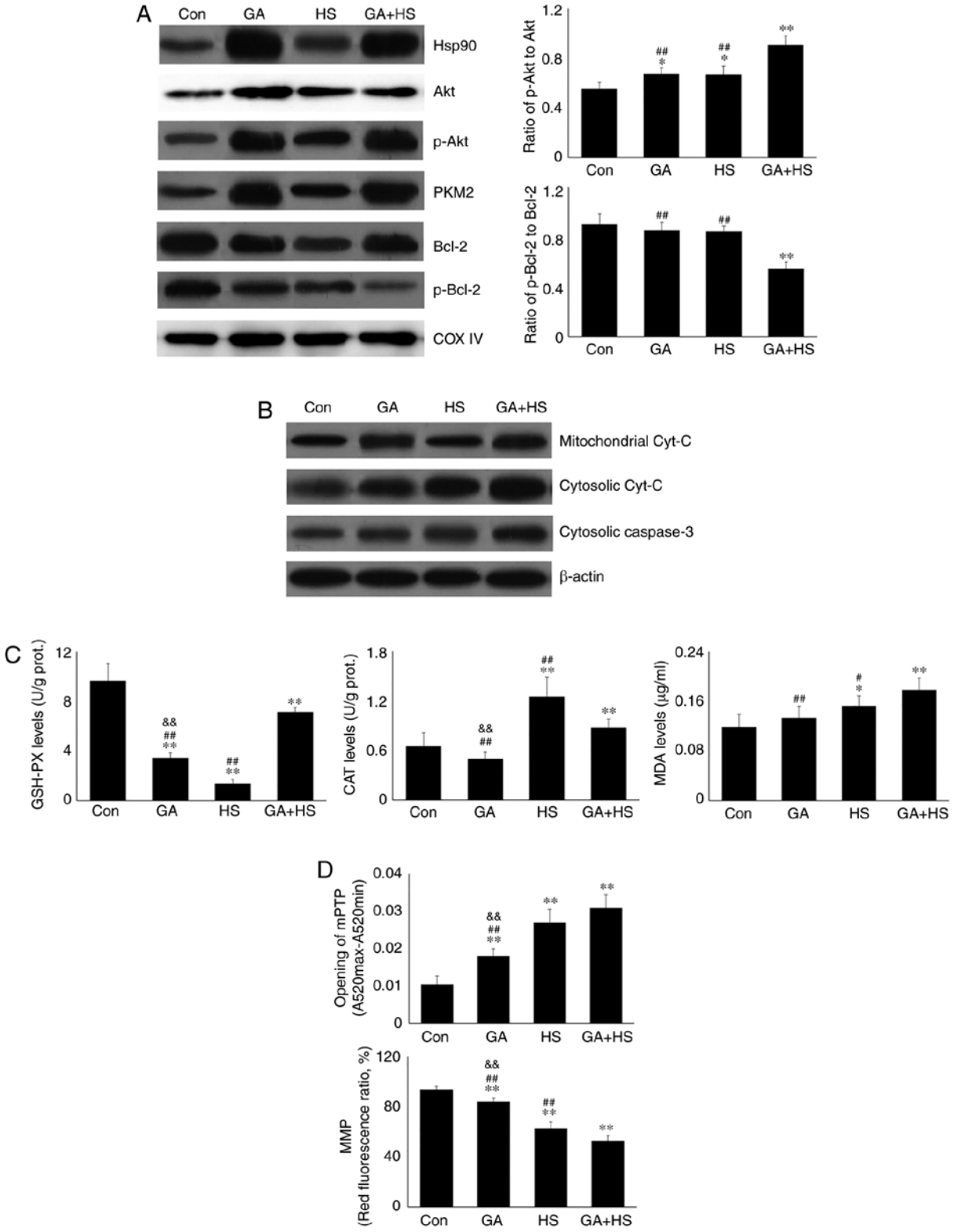

Figure 6. Effect of Hsp90 functional inhibition on the mitochondrial and cytosolic levels of Hsp90 and associated proteins, and the oxidation levels and function of myocardial mitochondria. (A) Representative western blotting results of mitochondrial Hsp90, Akt, p-Akt, PKM2, Bcl-2 and p-Bcl-2 are shown, and the ratios of phosphorylated/total protein abundance are also presented. (B) Representative western blotting results of mitochondrial cyt *c*, and cytosolic cyt *c* and caspase-3 are shown. (C) Effects of Hsp90 functional inhibition on the oxidation levels of myocardial mitochondria. (D) Effects of Hsp90 functional inhibition on the myocardial mitochondria. The relative abundance of all proteins was normalized to that of β-actin. All the results are expressed as the mean ± SD; n=5. *P<0.05 and **P<0.01 vs. Con, $^{\#}$P<0.05 and $^{\#\#}$P<0.01 vs. ASA + HS, and the comparison between ASA and HS is indicated by $^{\&\&}$P<0.01.

the mitochondrial and cytosolic cyt *c* levels simultaneously. Furthermore, GA did not markedly influence the oxidation and antioxidation indices. Compared with the HS group, GA followed by HS markedly stimulated the mitochondrial GSH-PX and MDA activities (Fig. 6C). GA promoted the opening of the mPTP and decreased the MMP (Fig. 6D).

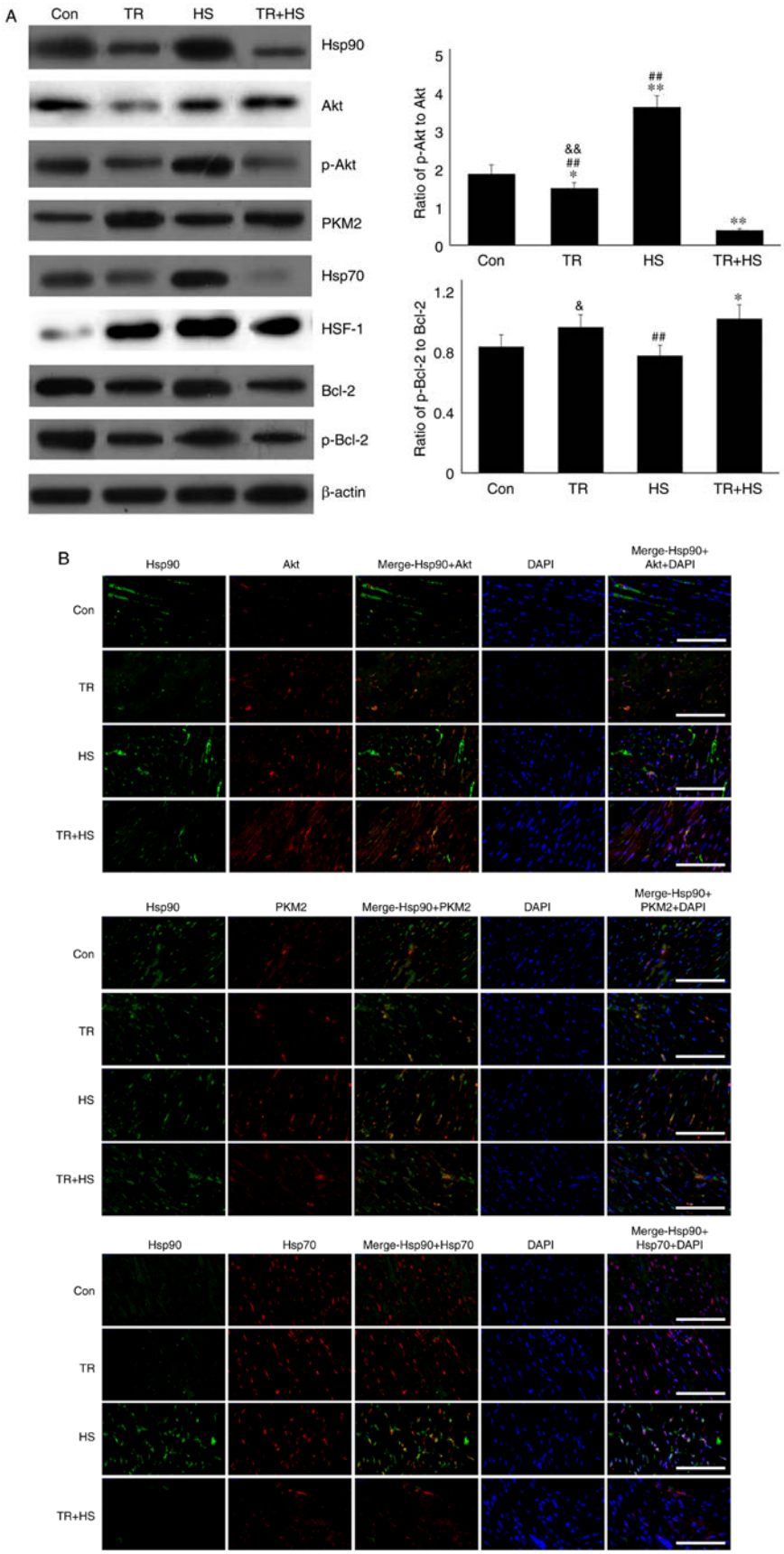

Figure 7. Effect of Akt activation inhibition on the levels of Hsp90, its associated proteins, and the co-localization of Hsp90 with tested client proteins. (A) Representative western blotting results of Hsp90, Akt, p-Akt, PKM2, Hsp70, HSF-1, Bcl-2 and p-Bcl-2 in the tested myocardial tissues, and the ratios of phosphorylated/total protein abundance. (B) Representative immunohistofluorescence staining images showing the interaction of Hsp90 with Akt, PKM2 and Hsp70 (Hsp90, green fluorescence; Akt/PKM2/Hsp70, red fluorescence; nucleus, blue fluorescence; the merged image of Hsp90 and Akt/PKM2/Hsp70 in the cytoplasm, yellow fluorescence; the merged of Hsp90 and Akt/PKM2/Hsp70 in the nucleus, white fluorescence) in myocardial tissues. Scale bar=100 μm. The relative abundance of all proteins was normalized to that of β-actin. All the results are expressed as the mean ± SD; n=5. *P<0.05 and **P<0.01 vs. Con, $^{\#\#}$P<0.01 vs. ASA + HS, and the comparison between ASA and HS is indicated by $^{\&}$P<0.05 and $^{\&\&}$P<0.01.

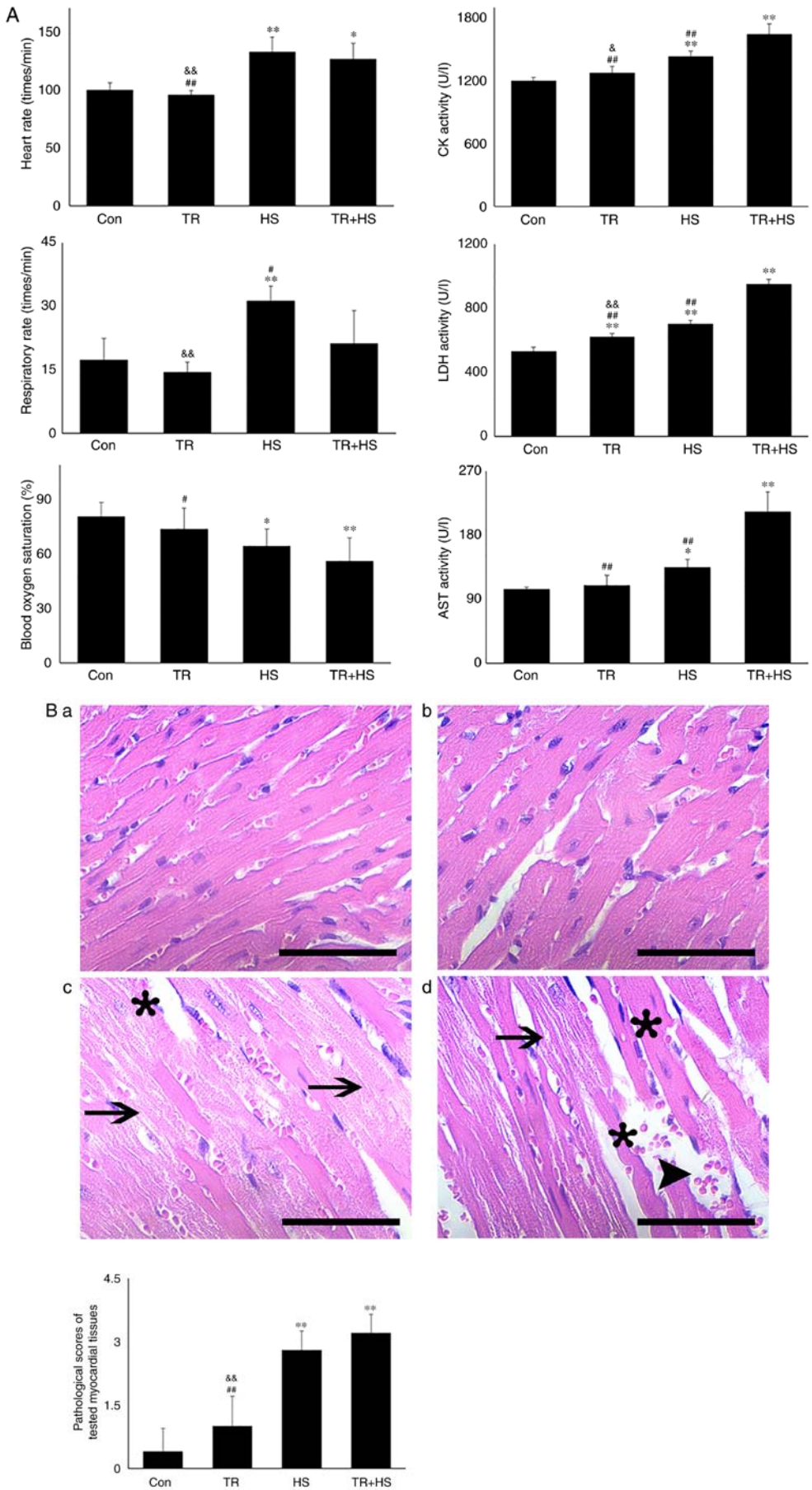

Figure 8. Effect of Akt activation inhibition on the levels of myocardial injury and cell apoptosis. (A) The changes in the heart rate, respiratory rate, blood oxygen saturation and serum enzymes levels in response to TR. (B) Representative H&E staining images of experimental mouse heart tissues and pathological scores. Panels a-d represent the Con, TR, HS, and TR + HS groups, respectively. Arrows indicate swelling cells and degeneration, arrowheads point to hemorrhage, and asterisks mark necrosis and myofiber rupture. Scale bar=100 μm.

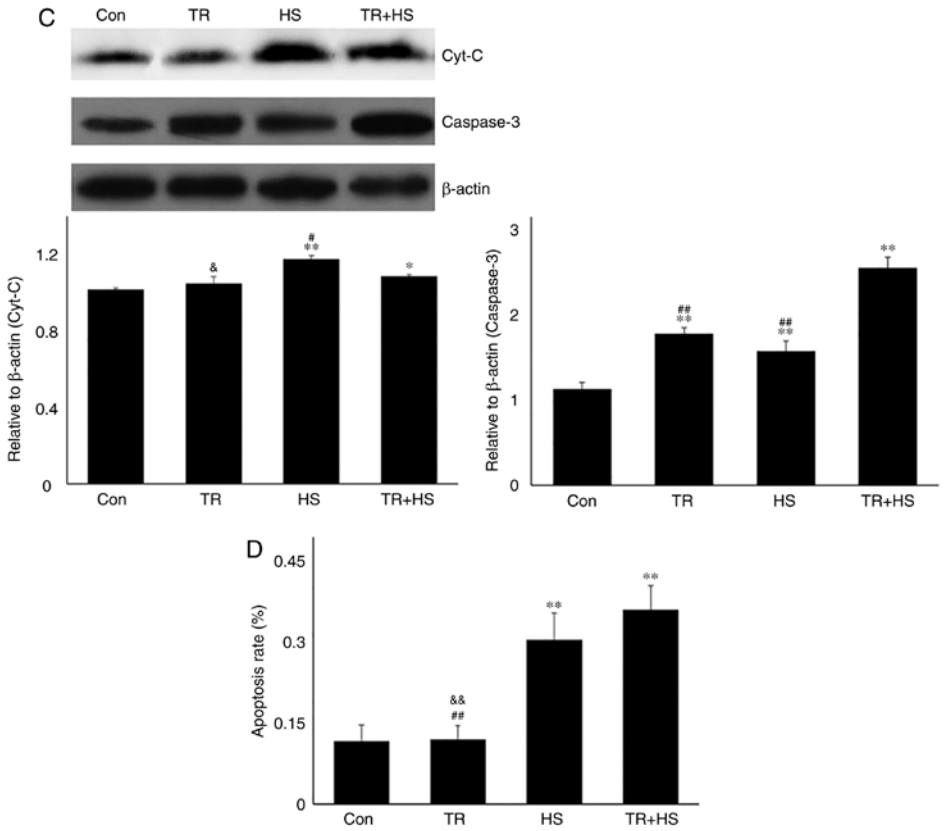

Figure 8. Continued. Effect of Akt activation inhibition on the levels of myocardial injury and cell apoptosis. (C) Effect of Akt activation inhibition on the cyt *c* and caspase-3 levels in heart tissues. (D) The apoptotic rate of myocardial cells under different treatments. The relative abundance of all proteins was normalized to that of β-actin. All the results are expressed as the mean ± SD; n=5. *P<0.05 and **P<0.01 vs. Con, $^{\#}$P<0.05 and $^{\#\#}$P<0.01 vs. ASA + HS, and the comparison between ASA and HS is indicated by $^{\&}$P<0.05 and $^{\&\&}$P<0.01.

Compared with the HS group, GA followed by HS further promoted mPTP opening and lowered the MMP (P<0.01). These results indicated that inhibition of Hsp90 could aggravate HS-induced mitochondrial damage by restricting Bcl-2 activity.

Inhibition of Akt activation exacerbates the damage to mouse hearts. The aforementioned results demonstrated that Hsp70 and HSF-1 levels increased after the inhibition of Hsp90, regardless of HS, suggesting that in the absence of Hsp90 function, Akt was probably activated by an alternative pathway and increased Hsp70 levels served to regulate the Hsp90 function. To confirm the hypothesis and its association with PKM2 *in vivo*, the Akt phosphorylation inhibitor TR was used to restrict the production of p-Akt in mouse myocardial tissues. Western blotting (Fig. 7A) revealed that, compared with that in the Con group, TR alone slightly decreased the Akt level, but significantly decreased the p-Akt, Bcl-2 and p-Bcl-2 levels, and decreased the ratio of p-Akt to Akt, accompanied by a decrease in Hsp90. HS following TR treatment further decreased the levels of Hsp90, p-Akt, Bcl-2 and p-Bcl-2, but increased the non-phosphorylated Akt level (thereby causing further decrease in the ratio of p-Akt to Akt), while HS alone could induce a high level of Hsp90 (compared with the Con group). Compared with that in the Con group, the PKM2 level increased in the TR group, while that in the TR + HS group was higher than that in the HS group. This may be responsible for the increase in the ratio of p-Bcl-2 to Bcl-2. Compared with that in the Con group, the HSF-1 level increased following TR treatment; however, it was not translocated into the nucleus to exert its function, particularly considering that Hsp70 levels were not increased in the TR group. Compared with the high level of HSF-1 in the HS group, in the TR + HS group, the HSF-1 level notably decreased, accompanied by the sharp downregulation of Hsp70 synthesis.

Immunohistofluorescence detection (Fig. 7B) revealed that the co-localization of Hsp90 and Akt increased in TR-treated heart tissues, and was mainly distributed in the cytoplasm of myocardial cells. Compared with that in the HS group, the co-localization between Hsp90 and Akt was reduced in the TR + HS group. The co-localization of Hsp90 and PKM2 in the TR group was observed primarily in the cytoplasm. The merged signal of Hsp90 and PKM2 could still be detected in the TR + HS group, but was not increased compared with that in the TR group. The co-localization of Hsp70 and Hsp90 in the TR and TR + HS groups was not observed, considering the decrease in the Hsp70 and Hsp90 signals.

As demonstrated in Fig. 8A, TR alone did not alter the heart rate, respiratory rate and blood oxygen saturation. Furthermore, compared with those induced by TR alone, HS following TR administration further increased the heart rate (P<0.01) and decreased blood oxygen saturation (P<0.01). Biochemical detection revealed that TR significantly upregulated the serum LDH level, but had no effect on CK and AST. HS exposure following TR significantly increased the activities of CK, LDH and AST (P<0.01), compared with those in the TR or HS groups. Pathological examination revealed that the injury

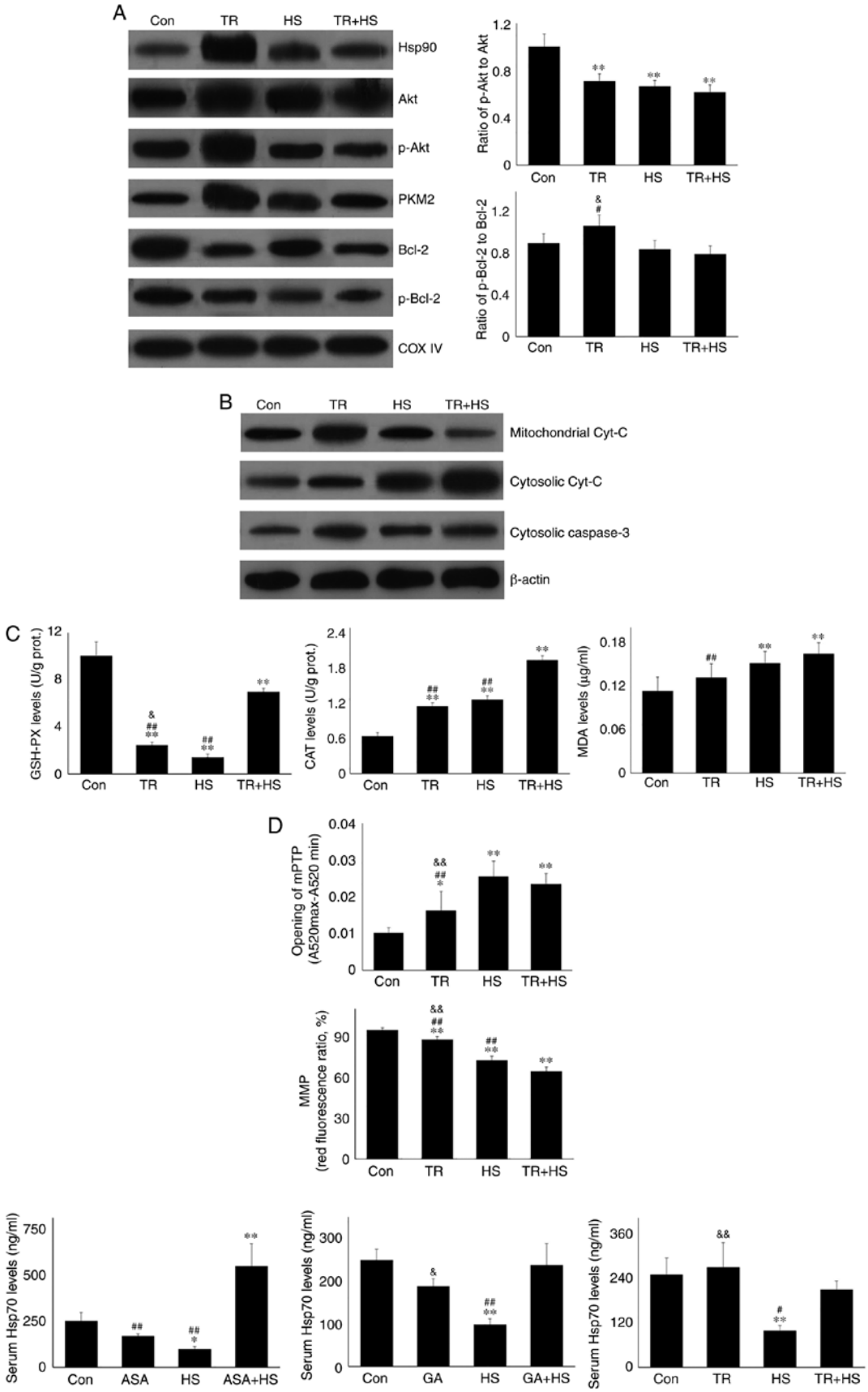

Figure 9. Effect of Akt activation inhibition on the mitochondrial and cytosolic levels of Hsp90 and associated proteins, the oxidation levels and function of myocardial mitochondria, and different treatments on the serum levels of Hsp70 in the tested mice. (A) Representative western blotting results of mitochondrial Hsp90, Akt, p-Akt, PKM2, Bcl-2 and p-Bcl-2. (B) Representative western blotting results of mitochondrial cyt *c*, and cytosolic cyt *c* and caspase-3. (C) Effects of Akt activation inhibition on the oxidative levels of myocardial mitochondria. (D) Effects of Akt activation inhibition on the opening of mPTP, and MMP of myocardial mitochondria, respectively. (E) Effects of different treatments on the serum levels of Hsp70 in the tested mice. The relative abundance of all proteins was normalized to that of β-actin. All the results are expressed as the mean ± SD; n=5. *P<0.05 and **P<0.01 vs. Con, $^{\#}$P<0.05 and $^{\#\#}$P<0.01 vs. ASA + HS, and the comparison between ASA and HS is indicated by $^{\&}$P<0.05 and $^{\&\&}$P<0.01.

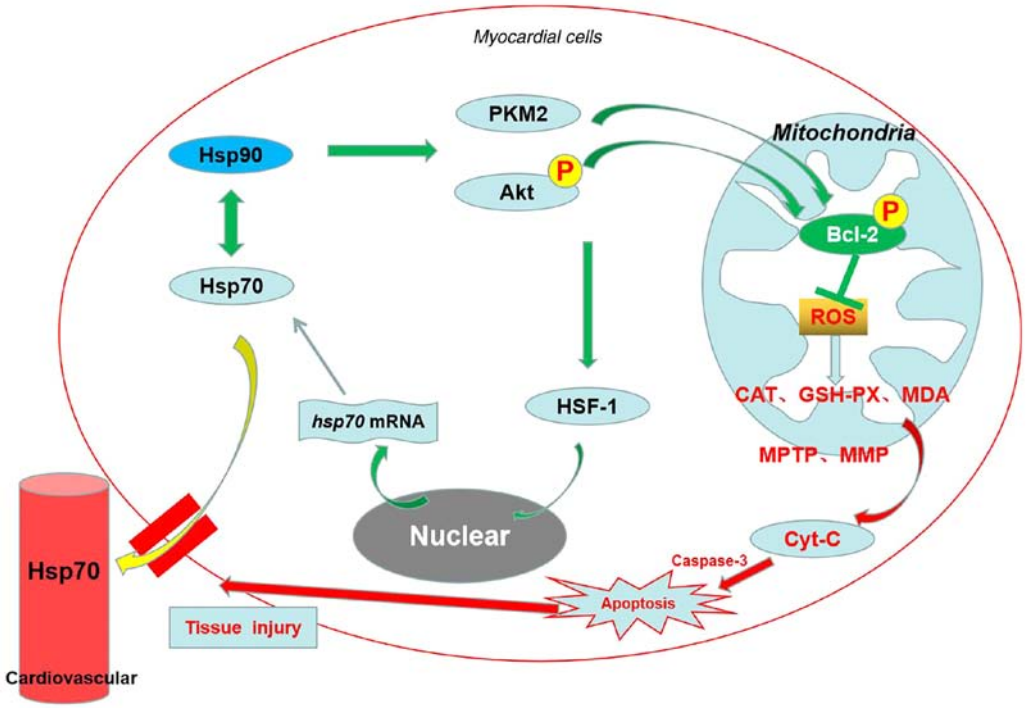

Figure 10. Schematic diagram summarizing the protective effects of Hsp90 against heat stress injury of myocardial tissues via the activation of Akt and PKM2 signaling. The *in vivo* experiments showed that Hsp90 promotes Akt phosphorylation, its mitochondrial translocation, and PKM2 mitochondrial translocation, thereby increasing the downstream the levels of mitochondrial Bcl-2 and its phosphorylation. This contributes toward the preservation of cardiac function and mitochondrial homeostasis, and the alleviation of oxidative stress and apoptosis in heat-stressed cardiomyocytes. Furthermore, several pathways that include Hsp90 can activate Akt signaling and then regulate the levels Hsp70 through HSF-1. Hsp70 interacts with Hsp90 to influence its downstream proteins. Myocardial Hsp70 can leak out into the bloodstream to initiate another protective mechanism.

score following TR treatment was slightly higher than that in the Con group, while the score in the TR + HS group was slightly higher than that in the HS group (Fig. 8B). In Fig. 8C, the cyt *c* level in the TR + HS group was significantly increased compared with that in the Con group, but was lower than that in the HS group ($P<0.05$). In addition, the caspase-3 levels in the TR + HS group were significantly higher than those in the HS group ($P<0.01$). Compared with that in the HS group, the apoptotic rate of myocardial cells in the TR + HS group was further stimulated in the tested hearts (Fig. 8D).

These findings indicated that under conditions of high Hsp90 levels induced by HS, inhibiting Akt activation markedly decreased the Bcl-2 level and its phosphorylation, thereby inducing more serious myocardial injury.

PKM2 cannot compensate the deletion of mitochondrial protection caused by inhibition of Akt activation. As shown in Fig. 9A, compared with that in the Con group, TR caused more Hsp90, Akt, and p-Akt to move into mitochondria, but more decrease of the ratio of p-Akt to Akt. It implied that when the levels of survival molecules in myocardial cells were insufficient, mitochondria were protected preferentially. However, the levels of mitochondrial Hsp90, Akt, and p-Akt in the TR + HS group were significantly lower ($P<0.01$) than those in the TR and HS groups, including the ratio of p-Akt to Akt. Furthermore, compared with those in the Con group, the Bcl-2 and p-Bcl-2 levels decreased following TR treatment, with and without HS treatment, and their levels in the TR + HS group were lower than those in HS group. The ratio of mitochondrial Bcl-2 and p-Bcl-2 was not significantly altered by TR treatment, as in the HS alone group. As shown in Fig. 9B, TR exposure stimulated the synthesis of mitochondrial cyt *c*, which leaked out of the mitochondria in the TR + HS group. The level of cytosolic cyt *c* was not influenced by TR alone, but was upregulated following subsequent HS exposure. Mitochondrial biochemistry analysis (Fig. 9C) revealed that GSH-PX activities in the TR, HS and TR + HS groups all decreased. TR increased the CAT level, but not that of MDA. HS following TR further induced CAT ($P<0.01$) and MDA levels, compared with those in the HS group. Mitochondrial function detection (Fig. 9D) demonstrated that TR alone increased mPTP opening and decreased the MMP. HS following TR induced a further decrease in the MMP compared with that in the HS group.

These results suggested that inhibition of Akt phosphorylation could further intensify mitochondrial injury of heat-stressed myocardial cells by inhibiting mitochondrial Bcl-2 and its phosphorylation, even though PKM2 exerted its normal function on Bcl-2.

Hsp90 expression promotes Hsp70 entry into blood to improve cardiovascular function. Serum Hsp70 was also detected in the present study. As shown in Fig. 9E, ASA, GA or TR alone did not alter the level of serum Hsp70 significantly, which contrasted with its significant downregulation by HS ($P<0.01$ or $P<0.05$). Notably, ASA markedly increased the serum Hsp70 level of heat-stressed mice in the ASA + HS group, while GA and TR did not, implying that increasing the serum Hsp70 level may be another method by which ASA protects the heat-stressed heart.

Discussion

Cardiomyocytes are engaged continuously in generating the powerful contractile force to pump blood to the whole body, and heat stress can lead to a surge in metabolic demand, followed by functional and structural disruption of these cells, resulting in heart failure (31,32). Our previous *in vivo* and *in vitro* studies confirmed that Hsp90 levels were high during heat stress, and were closely associated with resisting heat stress damage to the heart (8,19). However, the underlying mechanism of how Hsp90 exerts these effects remains elusive. In the present study, high levels of Hsp90 were observed in heat-stressed heart tissues, and ASA, an effective inducer of HSP90, was used to further enhance HSP90 levels to investigate its signaling pathways. The higher Hsp90 levels induced by ASA significantly reversed the HS-induced myocardial injury and increased blood oxygen saturation effectively by regulating the heart rate. Further investigation revealed that, during HS, higher Hsp90 levels were accompanied by higher levels of Akt and its phosphorylated version in cardiac tissue. The interaction of Akt with Hsp90 is necessary to activate Akt, which works on downstream survival signal proteins (33). Consistently, in the present study, ASA treatment also stimulated the interactive co-localization of Hsp90 and Akt, and promoted the nuclear translocation of Hsp90 in myocardial cells. Activated Akt functions to resist cellular oxidative stress and then inhibit apoptosis, mainly through its regulation of Bcl-2 (34,35). We hypothesized that the decrease in the ratio of p-Akt to Akt in myocardial tissue in the ASA treatment groups was mainly due to effective chaperone protection of higher Hsp90 on more Akt proteins. Meanwhile, PKM2 levels were upregulated in response to the Hsp90 inducer, ASA. Evidence suggests that the ATPase activity of Hsp90 facilitates the interaction between PKM2 and Bcl-2, and then phosphorylates Bcl-2 (15). Co-localized interaction is also necessary for Hsp90 to exert its auxiliary function on the target complex (36). The immunohistofluorescence analysis of the present study also showed that higher Hsp90 levels after ASA treatment strengthened the interaction between Hsp90 and PKM2.

The present study also revealed that, although Bcl-2 levels were decreased, the p-Bcl-2 levels and the ratio of p-Bcl-2 to Bcl-2 in the ASA and ASA + HS groups were increased compared with those in the Con and HS groups, respectively. This indicated that the activation of Bcl-2 was promoted by the Hsp90-Akt-p-Akt and Hsp90-PKM2 axes, which contradicted a previous study demonstrating that the Bcl-2 level should match the increase in Akt activation (37). Bcl-2 acts as a nodal point at the convergence of multiple pathways to inhibit apoptosis in peroxidized cells, particularly in the protection of mitochondrial structure and function (38,39). In mitochondria, Bcl-2 phosphorylation prevents the binding of Cul3-based E3 ligase to Bcl-2, thereby enhancing cellular resistance to oxidative stress (15).

In myocardial cells, mitochondria constitute ~45% of the volume and manufacture ~90% of the ATP, and myocardial tissue is particularly sensitive to free radicals due to its low levels of antioxidant enzymes (40,41). Stress-induced ROS generation causes mitochondrial dysfunction, resulting in irreversible myocardial oxidative injury (40,42). Heat stress markedly increased the degree of mitochondrial peroxidation and decreased the GSH-PX activities, thereby disturbing the mitochondrial structure and function, characterized by the increased opening of mPTP and the decreased MMP. These adverse conditions were significantly reversed by the higher Hsp90 levels resulting from ASA pre-treatment, confirming a positive role of Hsp90 in HS-induced myocardial mitochondria injury (43). Mitochondrial-dependent intrinsic apoptosis of cardiomyocytes is initiated by the leakage of mitochondrial cyt *c* and initiation of caspase-3, and is the main cause of myocardial damage, including myofiber loss and cardiac dysfunction (8,44). The results of the present study indicated that higher Hsp90 levels could inhibit HS-induced apoptosis by decreasing caspase-3 levels in cardiac tissue.

Hsp90 also serves a key role in protein mitochondrial translocation (45). The results of the present study showed that increased mitochondrial Hsp90 protein further increased the total amount of mitochondrial PKM2, Akt and p-Akt during heat stress, including the ratio of mitochondrial p-Akt to Akt. The stronger cytoplasmic co-localization of Akt/PKM2 with higher Hsp90 levels may suggest that mitochondrial translocation of Akt and PKM2 is completed with the assistance of Hsp90. This is in accordance with the results of another study on hypothermic preservation of rat hearts (21). The low levels of mitochondrial Bcl-2 during exposure to HS were partially reversed by the increased level of mitochondrial Hsp90 in the ASA + HS group, making them beneficial for the production of p-Bcl-2. Based on this increased protection from Bcl-2 and the consumption of p-Bcl-2 on the mitochondrial structure, mitochondrial cyt *c* could not leak into the cytoplasm to initiate caspase-3 dependent apoptosis. These all originated from the regulation of Hsp90 on PKM2 and Akt, and enabled protection of the myocardium via decreasing apoptosis.

In addition, the Akt pathway regulates the expression and nuclear translocation of HSF-1, followed by constitutive and inducible Hsp70 expression (28). Furthermore, Hsp70 serves an essential role in the substrate-loading phase of the chaperone function of Hsp90 by interacting functionally with the Hsp90-complex (46). Consistent with the aforementioned studies, the results of the present study also demonstrated that a higher level and activation of Akt, including its nuclear import in the ASA + HS group, induced HSF-1 and Hsp70 expression, followed by an increase in the co-localization between Hsp70 and Hsp90, which critically contributes toward the chaperone function of Hsp90 in myocardial cells.

To confirm the aforementioned effect of Hsp90, GA was used to inhibit its chaperone function *in vivo*. Previous studies have indicated that GA did not alter Hsp90 levels, but stimulated HSF-1 nuclear translocation and Hsp70 expression (20,29,30). Activated HSF-1 in the nucleus can stimulate the transcription of the *HSP70* gene (47). Consistently, the present study demonstrated that GA alone did not influence the Hsp90 level, but increased the levels of Hsp70 and HSF-1. In addition, the ratio of p-Akt to Akt and co-localization of Hsp90 with PKM2 and Hsp70 were all decreased. These results proved that GA effectively inhibited the function of Hsp90, which resulted in accumulation of Akt and PKM2 in myocardial tissues, thereby decreasing the ratio of p-Akt to Akt, and slightly strengthening the fake merge signal of Hsp90 and Akt. Finally, the levels of Bcl-2 and p-Bcl-2 (the executors that protect myocardial cells) and the ratio of p-Bcl-2 and Bcl-2 were restricted effectively

with and without HS exposure, which indicated that the chaperone function of Hsp90 was required to assist Akt activation and p-Akt/PKM2-mediated phosphorylation of Bcl-2 to resist heat-stress damage. It was also found that when Hsp90 was functionally inhibited, mitochondrial p-Akt levels remained increased, including Akt and PKM2, even resulting in an increase in the ratio of p-Akt to Akt. This suggested that Hsp90 may serve an auxiliary role in their mitochondrial translocation, instead of being strictly required. However, Hsp90 remained necessary for p-Akt and PKM2 to regulate mitochondrial Bcl-2 and its phosphorylation, evidenced by the significant decrease in the ratio of mitochondrial p-Bcl-2 to Bcl-2, which was consistent with previous studies showing that Hsp90 altered the conformation of intermitochondrial client proteins (e.g., p-Akt and PKM2) and facilitated the interaction between them and Bcl-2 to inhibit Bcl-2 degradation and secondary apoptosis (15,22). Inhibition of Hsp90 by GA intensified the heat-stress damage to mitochondrial integrity, followed by apoptosis of myocardial cells, which resulted in more serious pathological injury, accompanied by lower blood oxygen saturation.

Based on the aformentioned results, the preferred target of Hsp90 should be p-Akt rather than Akt during heat stress. To confirm this hypothesis and clarify the cross-talk between Hsp90-Akt-Bcl-2 and Hsp90-PKM2-Bcl-2, Triciribine (TR) was used to inhibit the phosphorylation of Akt at amino acids 308 and 473 (48). TR is highly selective for Akt and does not inhibit the activation of other kinases, such as phosphatidylinositol 3 kinase and phosphoinositol-dependent kinase 1 (48). In the present study, although PKM2 exhibited higher expression and Hsp90 was extensively degraded in the TR and TR + HS groups, the inhibition of Akt activation by TR still significantly decreased the levels of Bcl-2 and p-Bcl-2. Additionally, HS aggravated this adverse impact, thereby exacerbating heat-stress-induced tissue injury, even though the ratio of p-Bcl-2 and Bcl-2 showed an increase. Previous studies have suggested that PKM2 is capable of phosphorylating proteins as a protein kinase, and PKM2-dependent Bcl-phosphorylation is required to sustain the Bcl-2 protein level (15,49). This indicated that during heat stress, p-Akt was necessary for Hsp90 to influence Bcl-2 and its phosphorylation, and the Hsp90-PKM2 axis functions independently, but was not sufficient enough to account for the deficiency in Akt signaling. In mitochondria, TR also decreased the p-Akt level and the ratio of mitochondrial p-Akt to Akt, and HS was further downregulated it. Furthermore, despite the large consumption of mitochondrial Hsp90 and PKM2, the reduction of the Bcl-2 and p-Bcl-2 levels was not reversed during heat stress, and the ratio of mitochondria p-Bcl-2 and Bcl-2 was also unaltered. The loss of protective Bcl-2 by TR treatment induced more severe intermitochondrial peroxidation and myocardial apoptosis and damage.

An *in vitro* study on multiple myeloma cells revealed substantial downregulation of HSF-1 upon PI3K inhibition, which was accompanied by strong downregulation of Hsp70 (28). Similarly, the downregulation of p-Akt by TR also abrogated the accumulation of Hsp70, particularly under HS. However, the present study also noted that HSF-1 levels increased following TR treatment, regardless of HS. Considering that HSF-1 performs its function in the nucleus (20), and the fluorescence signal of nuclear Akt was weakened in the TR and TR + HS groups, the results suggested that Akt signaling may also be the regulator of the nuclear translocation of HSF-1, and that its expression could be affected by other factors. A previous study showed that pharmacological inhibition of Hsp90 strongly induced Hsp70, and the HSF-1-dependent induction of Hsp70 is controlled by PI3K (28). Consistently, Hsp70 was upregulated by GA in the present study. However, the activation of the Akt signaling pathway, as represented by the p-Akt level, remained at a high level. Therefore, an alternative way to activate Akt should exist *in vivo*, and remains to be further studied.

In addition, previous studies have confirmed that extracellular Hsp70 exists in patients with arthritis, atherosclerosis or other diseases, and is associated with the disease severity (50,51). However, the source of extracellular and serum Hsp70 remains unclear. The present study analyzed serum Hsp70 levels in the experimental mice and found that HS followed by ASA could significantly stimulate the serum Hsp70 level. This suggested that HS damages the myocardial cell membrane and causes intracellular Hsp70 to flow into the blood (51,52). At this point, Hsp70 acts as a cytokine, rather than a molecular chaperone, and combines with Toll-like receptor (TLR)-4 on the myocardial cell membrane, which activates downstream effectors to initiate the transcription of cytokine genes (e.g., those encoding tumor necrosis factor-α, interleukin-1, -6, -8 and -12) and accessory adhesion molecules (CD80 and CD86), which are important self-protective cellular factors (52). The results of the present study also showed that inhibition of Akt activation restricted serum Hsp70 levels by downregulating intracellular Hsp70. However, the increase in intracellular Hsp70 induced by GA did not cause upregulation of serum Hsp70, but the mechanism underlying this requires further investigation. Furthermore, PI3K-Akt is also a known classic autophagy pathway; therefore, the association between Hsp90 and mitochondrial autophagy should be further investigated in future experiments.

Taken together, as shown in Fig. 10, the results of the present study provided *in vivo* mechanistic evidence that Hsp90 acts as a myocardial protective molecule against heat-stress-induced apoptosis and damage via the Akt-Bcl-2 and PKM2-Bcl-2 survival signaling pathways at the cellular and mitochondrial levels, which contributes toward preserving cardiac function and mitochondrial homeostasis, thereby alleviating oxidative stress. The two signaling pathways act independently, and the former is predominant. Furthermore, the serum Hsp70 that leaks from myocardial cells may also participate in resisting heat stress. However, the present result would preferably be verified using a specific inducer of Hsp90, as there are multi-target effects of ASA. Therefore, identifying a specific Hsp90 agonist or developing a gene transfection method would be beneficial in a future *in vivo* study on heat stress. In conclusion, the present study may serve as a foundation for further investigation of the protection offered by Hsp90 induction against heat-stress damage, and identifies several novel potential targets to develop drugs that protect against heat stress.

Acknowledgements

Not applicable.

Funding

The present study was supported by grants from the National Natural Science Foundation Youth Funding Project of China (grant no. 31802157), the Postdoctoral Science Foundation of Jiangsu Province (grant no. 2018K206C), the National Natural Science Foundation of China (grant no. 31672520), and the Initial Scientific Research Fund of Young Teachers in Nanjing Agricultural University.

Availability of data and materials

The datasets used and/or analyzed during the current study are available from the corresponding author upon reasonable request.

Authors' contributions

XHZ and EDB were involved in developing the concept and design of the study. XHZ, JXW, JZS, BY and JRS performed the experiments. XHZ analyzed the data and prepared the manuscript. EDB revised the manuscript. All authors have read and approved the final version of the manuscript submitted for publication.

Ethics approval and consent to participate

All animal experiments were performed according to the guidelines of the regional Animal Ethics Committee and were approved by the Institutional Animal Care and Use Committee of Nanjing Agricultural University.

Patient consent for publication

Not applicable.

Competing interests

The authors declare that they have no competing interests.

References

1. Sandercock DA, Hunter RR, Nute GR, Mitchell MA and Hocking PM: Acute heat stress-induced alterations in blood acid-base status and skeletal muscle membrane integrity in broiler chickens at two ages: Implications for meat quality. Poult Sci 80: 418-425, 2001.
2. Bettaieb A and Averill-Bates DA: Thermotolerance induced at a fever temperature of 40 degrees C protects cells against hyperthermia-induced apoptosis mediated by death receptor signalling. Biochem Cell Biol 86: 521-538, 2008.
3. Herbst J, Gilbert JD and Byard RW: Urinary incontinence, hyperthermia, and sudden death. J Forensic Sci 56: 1062-1063, 2011.
4. Jones TS, Liang AP, Kilbourne EM, Griffin MR, Patriarca PA, Wassilak SG, Mullan RJ, Herrick RF, Donnell HD Jr, Choi K and Thacker SB: Morbidity and mortality associated with the July 1980 heat wave in St Louis and Kansas City, Mo. JAMA 247: 3327-3331, 1982.
5. Ghaznawi HI and Ibrahim MA: Heat stroke and heat exhaustion in pilgrims performing the Hajj (annual pilgrimage) in Saudi Arabia. Ann Saudi Med 7: 323-326, 1987.
6. Chang CP, Hsu YC and Lin MT: Magnolol protects against cerebral ischaemic injury of rat heatstroke. Clin Exp Pharmacol Physiol 30: 387-392, 2003.
7. Zak R: Development and proliferative capacity of cardiac muscle cells. Circ Res 35 (Suppl II): S17-S26, 1974.
8. Islam A, Lv YJ, Abdelnasir A, Rehana B, Liu ZJ, Zhang M, Tang S, Cheng YF, Chen HB, Hartung J and Bao ED: The role of Hsp90α in heat-induced apoptosis and cell damage in primary myocardial cell cultures of neonatal rats. Genet Mol Res 12: 6080-6091, 2013.
9. Yin B, Tang S, Sun J, Zhang X, Xu J, Di L, Li Z, Hu Y and Bao E: Vitamin C and sodium bicarbonate enhance the antioxidant ability of H9C2 cells and induce HSPs to relieve heat stress. Cell Stress Chaperones 23: 735-748, 2018.
10. Kregel KC: Heat shock proteins: Modifying factors in physiological stress responses and acquired thermotolerance. J Appl Physiol (1985) 92: 2177-2186, 2002.
11. Powers ET, Morimoto RI, Dillin A, Kelly JW and Balch WE: Biological and chemical approaches to diseases of proteostasis deficiency. Annu Rev Biochem 78: 959-991, 2009.
12. Sonna LA, Wenger CB, Flinn S, Sheldon HK, Sawka MN and Lilly CM: Exertional heat injury and gene expression changes: A DNA microarray analysis study. J Appl Physiol (1985) 96: 1943-1953, 2004.
13. Pérez-Salamó I, Papdi C, Rigó G, Zsigmond L, Vilela B, Lumbreras V, Nagy I, Horváth B, Domoki M, Darula Z, *et al*: The heat shock factor A4A confers salt tolerance and is regulated by oxidative stress and the mitogen-activated protein kinases MPK3 and MPK6. Plant Physiol 165: 319-334, 2014.
14. Fulda S and Debatin KM: Extrinsic versus intrinsic apoptosis pathways in anticancer chemotherapy. Oncogene 25: 4798-4811, 2006.
15. Liang J, Cao R, Wang X, Zhang Y, Wang P, Gao H, Li C, Yang F, Zeng R, Wei P, *et al*: Mitochondrial PKM2 regulates oxidative stress-induced apoptosis by stabilizing Bcl2. Cell Res 27: 329-351, 2017.
16. Evans M, Fored CM, Bellocco R, Fitzmaurice G, Fryzek JP, McLaughlin JK, Nyrén O and Elinder CG: Acetaminophen, aspirin and progression of advanced chronic kidney disease. Nephrol Dial Transplant 24: 1908-1918, 2009.
17. Wali RK: Aspirin and the prevention of cardiovascular disease in chronic kidney disease: Time to move forward? J Am Coll Cardiol 56: 966-968, 2010.
18. Amici C, Rossi A and Santoro MG: Aspirin enhances thermotolerance in human erythroleukemic cells: An effect associated with the modulation of the heat shock response. Cancer Res 55: 4452-4457, 1995.
19. Zhang XH, Zhu HS, Qian Z, Tang S, Wu D, Kemper N, Hartung J and Bao ED: The association of Hsp90 expression induced by aspirin with anti-stress damage in chicken myocardial cells. J Vet Sci 17: 35-44, 2016.
20. Zhang XH, Wu H, Tang S, Li QN, Xu J, Zhang M, Su YN, Yin B, Zhao QL, Kemper N, *et al*: Apoptosis in response to heat stress is positively associated with heat-shock protein 90 expression in chicken myocardial cells in vitro. J Vet Sci 18: 129-140, 2017.
21. Yu GW, Chen J, Chen YY, Zheng MZ and Shen YL: Heat-shock protein 90-dependent translocation of Akt to mitochondria mediates insulin-like growth factor 1-induced protection of rat hearts under hypothermic preservation. Chin J Pathophysiol 28: 1773-1778, 2012.
22. Sato S, Fujita N and Tsuruo T: Modulation of Akt kinase activity by binding to Hsp90. Proc Natl Acad Sci USA 97: 10832-10837, 2000.
23. Chrousus GP and Gold PW: The concepts of stress and stress system disorders. Overview of physical and behavioral homeostasis. JAMA 267: 1244-1252, 1992.
24. Laszlo A: The effects of hyperthermia on mammalian cell structure and function. Cell Prolif 25: 59-87, 1992.
25. Yatvin MB and Cramp WA: Role of cellular membranes in hyperthermia: Some observations and theories reviewed. Int J Hyperthermia 9: 165-185, 1993.
26. Li P, Nijhawan D, Budihardjo I, Srinivasula SM, Ahmad M, Alnemri ES and Wang X: Cytochrome c and dATP-dependent formation of Apaf-1/caspase-9 complex initiates an apoptotic protease cascade. Cell 91: 479-489, 1997.
27. Ahmad N, Wang Y, Haider KH, Wang B, Pasha Z, Uzun O and Ashraf M: Cardiac protection by mitoKATP channels is dependent on Akt translocation from cytosol to mitochondria during late preconditioning. Am J Physiol Heart Circ Physiol 290: H2402-H2408, 2006.
28. Chatterjee M, Andrulis M, Stühmer T, Müller E, Hofmann C, Steinbrunn T, Heimberger T, Schraud H, Kressmann S, Einsele H and Bargou RC: The PI3K/Akt signaling pathway regulates the expression of Hsp70, which critically contributes to Hsp90-chaperone function and tumor cell survival in multiple myeloma. Haematologica 98: 1132-1141, 2013.

29. Shen HY, He JC, Wang Y, Huang QY and Chen JF: Geldanamycin induces heat shock protein 70 and protects against MPTP-induced dopaminergic neurotoxicity in mice. J Biol Chem 280: 39962-39969, 2005.
30. Zhang H, Chung D, Yang YC, Neely L, Tsurumoto S, Fan J, Zhang L, Biamonte M, Brekken J, Lundgren K and Burrows F: Identification of new biomarkers for clinical trials of Hsp90 inhibitors. Mol Cancer Ther 5: 1256-1264, 2006.
31. Wu D, Xu J, Song E, Tang S, Zhang X, Kemper N, Hartung J and Bao E: Acetyl salicylic acid protected against heat stress damage in chicken myocardial cells and may associate with induced Hsp27 expression. Cell Stress Chaperones 20: 687-696, 2015.
32. Zhao B, Sun G, Feng G, Duan W, Zhu X, Chen S, Hou L, Jin Z and Yi D: Carboxy terminus of heat shock protein (HSP) 70-interacting protein (CHIP) inhibits HSP70 in the heart. J Physiol Biochem 68: 485-491, 2012.
33. Fontana J, Fulton D, Chen Y, Fairchild TA, McCabe TJ, Fujita N, Tsuruo T and Sessa WC: Domain mapping studies reveal that the M domain of hsp90 serves as a molecular scaffold to regulate Akt-dependent phosphorylation of endothelial nitric oxide synthase and NO release. Circ Res 90: 866-873, 2002.
34. Ikeyama S, Kokkonen G, Shack S, Wang XT and Holbrook NJ: Loss in oxidative stress tolerance with aging linked to reduced extracellular signal-regulated kinase and Akt kinase activities. FASEB J 16: 114-116, 2002.
35. Kaufmann T, Schlipf S, Sanz J, Neubert K, Stein R and Borner C: Characterization of the signal that directs Bcl-x(L), but not Bcl-2, to the mitochondrial outer membrane. J Cell Biol 160: 53-64, 2003.
36. Jackson S (ed): Molecular chaperones. Berlin Heidelberg, Springer-verlag, pp1-272, 2013.
37. Pugazhenthi S, Nesterova A, Sable C, Heidenreich KA, Boxer LM, Heasley LE and Reusch JE: Akt/protein kinase B up-regulates Bcl-2 expression through cAMP-response element-binding protein. J Biol Chem 275: 10761-10766, 2000.
38. Yip KW and Reed JC: Bcl-2 family proteins and cancer. Oncogene 27: 6398-6406, 2008.
39. Ling YH, Liebes L, Zou Y and Perez-Soler R: Reactive oxygen species generation and mitochondrial dysfunction in the apoptotic response to Bortezomib, a novel proteasome inhibitor, in human H460 non-small cell lung cancer cells. J Biol Chem 278: 33714-33723, 2003.
40. Govender J, Loos B, Marais E and Engelbrecht AM: Mitochondrial catastrophe during doxorubicin-induced cardiotoxicity: A review of the protective role of melatonin. J Pineal Res 57: 367-380, 2014.
41. Wang S, Wang Y, Zhang Z, Liu Q and Gu J: Cardioprotective effects of fibroblast growth factor 21 against doxorubicin-induced toxicity via the SIRT1/LKB1/AMPK pathway. Cell Death Dis 8: e3018, 2017.
42. Govender J, Loos B and Engelbrecht AM: Melatonin: A protective role against doxorubicin-induced cardiotoxicity. Future Oncol 11: 2003-2006, 2015.
43. Liu D, Ma Z, Di S, Yang Y, Yang J, Xu L, Reiter RJ, Qiao S and Yuan J: AMPK/PGC1α activation by melatonin attenuates acute doxorubicin cardiotoxicity via alleviating mitochondrial oxidative damage and apoptosis. Free Radic Biol Med 129: 59-72, 2018.
44. Priya LB, Baskaran R, Huang CY and Padma VV: Neferine ameliorates cardiomyoblast apoptosis induced by doxorubicin: Possible role in modulating NADPH oxidase/ROS-mediated NFκB redox signaling cascade. Sci Rep 7: 12283, 2017.
45. Fan AC, Bhangoo MK and Young JC: Hsp90 functions in the targeting and outer membrane translocation steps of Tom70-mediated mitochondrial import. J Biol Chem 281: 33313-33324, 2006.
46. Daugaard M, Rohde M and Jaattela M: The heat shock protein 70 family: Highly homologous proteins with overlapping and distinct functions. FEBS Lett 581: 3702-3710, 2007.
47. Chaudhury S, Welch TR and Blagg BSJ: Hsp90 as a target for drug development. ChemMedChem 1: 1331-1340, 2006.
48. Dieterle A, Orth R, Daubrawa M, Grotemeier A, Alers S, Ullrich S, Lammers R, Wesselborg S and Stork B: The Akt inhibitor triciribine sensitizes prostate carcinoma cells to TRAIL-induced apoptosis. Int J Cancer 125: 932-941, 2009.
49. Yang W, Xia Y, Hawke D, Li X, Liang J, Xing D, Aldape K, Hunter T, Alfred Yung WK and Lu Z: PKM2 phosphorylates histone H3 and promotes gene transcription and tumorigenesis. Cell 150: 685-696, 2012.
50. Johnson JD, Campisi J, Sharkey CM, Kennedy SL, Nickerson M and Fleshner M: Adrenergic receptors mediate stress-induced elevations in extracellular Hsp72. J Appl Physiol (1985) 99: 1789-1795, 2005.
51. Kumaraguru U, Pack CD and Rouse BT: Toll-like receptor ligand links innate and adaptive immune responses by the production of heat-shock proteins. J Leukoc Biol 73: 574-583, 2003.
52. Asea A, Kraeft SK, Kurt-Jones EA, Stevenson MA, Chen LB, Finberg RW, Koo GC and Calderwood SK: HSP70 stimulates cytokine production through a CD14-dependant pathway, demonstrating its dual role as a chaperone and cytokine. Nat Med 6: 435-442, 2000.